

When Externalities Collide: Influenza and Pollution

Joshua Graff Zivin*

UC San Diego & NBER

Matthew Neidell*

Columbia University & NBER

Nicholas J. Sanders*

Cornell University & NBER

Gregor Singer*

LSE

March 12th, 2022

Abstract

Influenza and air pollution each pose significant public health risks with global economic consequences. The common pathways through which each harms health presents a case of compounding risk via interacting externalities. Using instrumental variables based on changing wind directions, we first show that increased levels of contemporaneous pollution increase influenza hospitalizations. We then exploit random variations in the effectiveness of the influenza vaccine as an additional instrument to show vaccine protection neutralizes this relationship. Evidence suggests seemingly disparate policy actions of pollution control and vaccination campaigns interact with each other, and pollution exposure gaps help explain racial gaps in influenza incidence.

Keywords: air pollution, influenza, hospitalizations, vaccines, externalities

JEL codes: Q53, I12, I11

*Corresponding authors: Joshua Graff Zivin: University of California, San Diego, CA 92093, E-mail: jgraffzivin@ucsd.edu. Matthew Neidell: Columbia University, New York, NY 10027, E-mail: mn2191@cumc.columbia.edu. Nicholas J. Sanders: Cornell University, Ithaca, NY 14850, E-mail: njsanders@cornell.edu. Gregor Singer: London School of Economics, London WC2A 2AE, UK, E-mail: g.a.singer@lse.ac.uk. We thank Douglas Almond, Max Auffhammer, Luisa Osang, Jeffrey Shaman, four anonymous reviewers, the editor, and participants at seminars at the University of California Environmental Economics group, UCSD, LSE, Vanderbilt for helpful discussions. G.S. acknowledges support from the Grantham Research Institute on Climate Change and the Environment, at the London School of Economics, and the ESRC Centre for Climate Change Economics and Policy (CCCEP) (ref. ES/R009708/1). All errors are our own. The IRB for access to the HCUP data through the National Bureau of Economic Research (NBER) was approved by the NBER.

Influenza (flu) and air pollution are significant public health risks that impact nations around the world. The flu causes an estimated 3-5 million severe cases per year, and nearly half a million deaths (Lambert & Fauci 2010, Iuliano et al. 2018). Air pollution causes 4.5 million annual deaths (Cohen et al. 2017), with annual economic costs estimated to exceed \$US 800 billion in the U.S. alone (Putri et al. 2018, Tschofen, Azevedo & Muller 2019). While public health policies to address these issues are often considered in isolation, both share common etiological pathways through which they harm human health.

Interactions between the flu and pollution are an illustrative economic case of compounding risk from interacting externalities. Influenza is an infectious disease whereby the actions of one infected individual impose negative externalities on others by increasing risk of infection, while air pollution is a negative externality of economic activity. Our analysis demonstrates that policies to address these distinct externalities have significant interactive effects: the flu vaccine can protect against certain harms from air pollution, and reduced levels of air pollution lessen the harmful effects of influenza exposure. Thus, the seemingly disparate policy actions of pollution control and expanded vaccination may jointly provide greater returns than when studied in isolation.

We begin our analysis by exploring the relationship between air pollution and influenza. Exposure to air pollution can affect influenza severity (Jaspers et al. 2005, Lee et al. 2014) and, to a lesser degree, its spread (Chen et al. 2010). We extend the cross-sectional epidemiological literature¹ to establish a causal relationship between air pollution and flu cases. We use patient-level administrative data on inpatient hospitalizations from 2007-2017 across 21 U.S. states, which allows us to focus on cases with a definitive influenza diagnosis.² We estimate econometric models with spatial and temporal fixed effects to control for numerous unobservable factors, and build on the pioneering work of (Deryugina et al. 2019) by using plausibly exogenous variation in wind directions as an instrument for pollution. We find higher pollution levels significantly increase flu inpatient hospitalizations; a one-standard-deviation increase in the monthly Air Quality Index (10.9-unit increase in our data) amounts to approximately 35.7% additional flu-related inpatient hospitalizations in the U.S. during influenza season. Compared to the effect of air pollution on all respiratory hospitalizations, our findings suggest influenza accounts for around 18% of all air pollution-induced respiratory inpatient hospitalizations.

Next, we explore whether influenza vaccine protection, which we define as a combination of vaccine take-up and effectiveness, moderates the estimated relationship above. As vaccine take-up can be endogenous across both time and location, we instrument for vaccine protection using vaccine ef-

¹See, for example, Brauer et al. (2002), Wong et al. (2009), Chen et al. (2010), Liang et al. (2014) and the important economic history paper by Clay, Lewis & Severnini (2018). In a study of the Spanish flu in 1918, Clay, Lewis & Severnini (2018) show cities with higher coal-fired power generating capacity saw higher mortality rates, potentially through exposure to higher air pollution.

²Estimation based simply on physician encounters is more difficult, as influenza testing is not conducted systematically, and reporting of positive cases is not mandatory for this patient population.

fectiveness weighted by influenza-susceptibility (in addition to using our instrument for pollution). Effectiveness of the flu vaccine varies from year to year: producers forecast viral strain match months ahead of time, and antigenic drift or shift induces random deviations in realized match quality.³ This makes the random draw of the viral match orthogonal to unobserved determinants of health, allowing us to identify a causal relationship between the vaccine and health harms from pollution. The orthogonality of vaccine effectiveness also offers an additional test that pollution has a causal effect on flu admissions. If a vaccine designed specifically to protect against the flu diminishes the impact of pollution on influenza hospital admissions, then it must be the case that pollution contributes to influenza hospitalizations. When we include an interaction between air pollution and vaccine protection, we find that the flu vaccine offers significant protection from influenza-related costs of pollution.⁴ Vaccine protection levels close to the average across time in our sample fully neutralize the relationship between pollution and additional flu hospitalizations.

Given the unequal burden of both flu and pollution exposure across society, we also explore results by race and ethnicity. Both of our main findings – that air pollution increases flu hospitalizations and vaccine protection moderates this relationship – are consistent across these dimensions. Combined with evidence of significant differences in flu incidence and severity by race (e.g. [Quinn et al. 2011](#)), our results suggest that the well-established differences in ambient pollution concentrations across racial and ethnic groups (e.g. [Banzhaf, Ma & Timmins 2019](#), [Colmer et al. 2020](#), [Currie, Voorheis & Walker 2020](#)) serve as an important mechanism driving disparities in influenza outcomes across such groups. Moreover, since flu vaccines protect against some pollution-induced harms, our results imply that the private and external benefits from vaccines is considerably higher in communities disproportionately exposed to poor air quality.

An important feature of our context is that the spread of influenza and pollution are externalities. As externalities, they justify government intervention in the form of policies, such as increased vaccine take-up and improved air quality.⁵ The interaction of the two suggests that the seemingly disparate policy actions of pollution control and vaccination campaigns jointly provide greater returns than those implied by addressing either in isolation. A back of the envelope calculation suggests a 10% (3.5 AQI points) reduction in the AQI in an historically ineffective vaccine year (11% vaccine take-up adjusted for effectiveness) would avert 16.6% of all influenza-associated hospitalizations across the U.S. Meanwhile a 10% improvement in vaccine take-up at the average vaccine effectiveness (or, equivalently, a 10% improvement in vaccine effectiveness at the average vaccine take-up) in a historically polluted

³Other papers using similar variation include [Ward \(2014\)](#) and [White \(2019\)](#).

⁴Access to health care may ameliorate impacts of adverse environmental conditions more generally. [Mullins & White \(2020\)](#) show that better access to acute care can help protect against health harms from extreme temperature.

⁵A similar logic applies to the more difficult task of improving vaccine effectiveness. In that case, policies are more likely to utilize the standard push and pull mechanisms used to overcome the underinvestment problem that arises due to the public good nature of scientific knowledge ([Kremer & Williams 2010](#)).

year (38.2 AQI) would avert 34.6% of pollution-driven influenza hospitalizations. The optimal mix of these policies will depend on relative costs as well as the ‘spillover’ benefits each may generate beyond influenza.

The paper proceeds as follows. We begin by describing potential biological mechanisms and our data, and present why it is particularly well-suited to addressing the question of interacting externalities (Section I.). We then discuss our econometric model, and describe in detail the various instruments we use to address issues of endogeneity and measurement error (Section II.). After we present our main results and explore variations in our model assumptions, we discuss the implications of our findings, both in the context of our analysis and the larger question of social welfare maximization (Section III.), before we conclude (Section IV.).

I. Background and Data

A. Potential biological mechanisms

The primary channel through which air pollution could affect influenza hospitalizations is increasing severity of influenza. Like smoking (Han et al. 2019), air pollution can impair the respiratory functioning of patients, e.g., by damaging the respiratory epithelium, thereby facilitating the progression of influenza virus beyond the epithelial barrier into the lungs (Diamond, Legarda & Ryan 2000, Jaspers et al. 2005, Ciencewicki & Jaspers 2007, Rivas-Santiago et al. 2015). Existing medical research finds exposing *in vitro* respiratory epithelial cells to air pollution increases susceptibility and penetration of influenza (Jaspers et al. 2005), and experimental exposure of mice to air pollution before influenza infections increases morbidity and mortality (Hahon et al. 1985, Lee et al. 2014).

There is also some suggestive evidence that air pollution could affect influenza hospitalizations through modest increases in the spread of influenza. Like humidity and temperature (Lowen et al. 2007, Shaman & Kohn 2009, Shaman et al. 2010, Ijaz et al. 1985, Casanova et al. 2010), air pollution particles could extend the airborne survival of viruses outside the body (Ijaz et al. 1985, Tellier 2009, Chen et al. 2010, Khare & Marr 2015, Lou et al. 2017, Wolkoff 2018) and thus increase the probability of disease transmission.

B. Data

We combine data from multiple sources with health outcomes, pollution concentrations, vaccine information and weather variables.

Inpatient hospitalizations: Our primary health outcome is inpatient hospitalizations for influenza. We use patient-level data on inpatient hospitalizations from the Health Care and Utilization Project (HCUP 2018b). The HCUP data covers the universe of hospital admissions in the reporting states. While Medi-

care data, an alternative popular data source, covers the entire U.S., the advantage of the HCUP data is that it covers all age groups, not only the elderly. We focus on influenza cases by using patient level information on diagnosed diseases per International Classification of Diseases (ICD) codes.⁶ We limit analysis to data from 2007 to 2017, for which we also have detailed vaccine effectiveness data available. This gives us an unbalanced panel of 21 U.S. states, with an average of 5.5 years of observations per state (see Table A.1 in Appendix A.1 for details on data availability by state and year). Figure A.1 in the Appendix shows that the HCUP data is broadly representative of U.S. data by comparing distributions of several socio-demographic variables across counties in our HCUP data with distributions across all U.S. counties.

We define our outcome as the count of inpatient admissions per county-year-month where the ICD code indicates influenza.⁷ Given the presence of primary and secondary diagnosis codes, we conduct analyses using three possible classifications of flu admissions: (i) cases where the only diagnosis is influenza (most restrictive); (ii) cases where any diagnosis is influenza (least restrictive); and (iii) cases where the primary diagnosis is influenza. The third option reflects a middle ground which we use as our baseline outcome.

We focus on the influenza season, which the U.S. Centers for Disease Control and Prevention (CDC) defines as October to March, and explore results extending the season in Appendix A.3. Figure 1a shows the seasonality of inpatient hospitalizations in our data, which matches closely with general CDC-reported influenza-like illnesses (see Table A.2 in Appendix A.1). Based on month of admission and patient zip code, we aggregate hospitalization data to the county-year-month level and assign a zero value to counties in months with no reported influenza admission, conditional on reporting data in the given year.⁸ During the influenza season, 54% of county-year-months have no reported influenza-related hospital admissions in the HCUP data, and our results are robust to inclusion or exclusion of zero valued county-year-months. To compare our main results with the more general effect of air pollution on any respiratory hospitalization (including influenza), we also construct a variable that contains the count of inpatient hospitalizations where the primary diagnosis is any respiratory diagnosis.⁹ Finally, for a falsification test we use primary ICD codes associated with osteoarthritis as an outcome variable, which is unlikely to be affected by air quality and influenza.¹⁰

⁶We exclude patients whose zip code is from a different state than the hospital in which they are treated.

⁷We use the Clinical Classifications Software (CCS) from the Agency for Healthcare Research and Quality (AHRQ) to classify relevant influenza ICD codes. These are all 5-digit ICD codes grouped under the following 3-digit ICD-9-CM codes: 487, 488; and, for the period from October 2015 when the system was changed to ICD-10-CM, the following 3-digit ICD-10-CM codes: J09, J10, J11.

⁸Put another way, we only impute zeros for counties and year-months in states that report data in that given year but have zero influenza hospitalizations in a given month. We use the crosswalk from zip codes to counties from the U.S. Department of Housing and Urban Development (Din & Wilson 2020).

⁹These are all 5-digit ICD codes grouped under the following 2-digit ICD-9-CM codes: 46, 47, 48, 49, 50, 51; and the following 2-digit ICD-10-CM code: J0, J1, J2, J3, J4, J5, J6, J7, J8, J9.

¹⁰Osteoarthritis consists of all 5-digit ICD codes grouped under the following 3-digit ICD-9-CM codes: 715, V134; and the

Air quality: As our measure of pollution, we begin with the U.S. Environmental Protection Agency’s (EPA 2020) Air Quality Index (AQI) at the county-day level, which we aggregate to county-by-year-by-month to match hospitalization outcomes.¹¹ We focus on the AQI as a summary measure of overall air quality, based on the primary criteria pollutants specified in the Clean Air Act.¹² We do so as the high degree of correlation between several individual pollutants makes it challenging to separately identify the effect of each pollutant independently. We note that most of the “forcing” pollutant that drives variation in the AQI in our setting is PM2.5.

Weather, wind directions and inversions: To address weather as a confounder, we use monthly weather averages from Xia et al. (2012), Mocko & NASA/GSFC/HSL (2012), including temperature, specific humidity, vertical and horizontal wind speed, and precipitation at the 0.125 by 0.125 degree level, all aggregated up to the county-by-year-by-month level.

To construct our main instrument for pollution, we construct wind direction for a county-year-month by taking the average horizontal (u_i) and vertical (v_i) wind components from the monthly raw data and calculating the average angle the wind is blowing from as $WDIR_i = 180/\pi \arctan 2(-u_i, -v_i)$.¹³

Temperature inversions can also influence ground-level pollution levels (Arceo, Hanna & Oliva 2016), which allows us to use inversions as an additional pollution instrument. To calculate inversions, we use daily three-dimensional temperature averages between midnight and 6AM at each location on each day from GMAO (2015), regrided to the 0.25 by 0.25 degree level. We use the difference in temperature between the two pressure levels closest to the surface at each location, and average this difference up to the county-day level. We then calculate the share of days with inversions in a county-year-month as the share of days when the difference between the layer further away from the surface and the layer closest to the surface is positive, i.e., the temperature rises with altitude. We calculate the average strength of inversion in a county-year-month as the average difference in temperature between the two altitude levels on the days where inversions are present.

Vaccine take-up and effectiveness: We obtain average vaccine take-up rates (VR) by state, season, and age group or racial group from CDC (2008, 2009, 2015, 2020), Lu et al. (2013), Schiller & Euler (2009). Figure 1b shows that on average, vaccine take-up is highest among those 65 years and older or those 8 years and younger. Figure A.4a in Appendix A.1 shows temporal variation in vaccine take-up rates

following 3-digit ICD-10-CM code: M15, M16, M17, M18, M19. We also show effects for all disease groupings as additional robustness checks in the Appendix.

¹¹The EPA pre-aggregates data to the daily county level in the case of multiple monitors per county. For missing county-year-months, we take the average value of the adjacent counties in the same month. We winsorize the AQI at the top and bottom 1% for the main analysis, and show robust results to both data cleaning choices in Appendix A.3.

¹²The AQI captures pollution from particulate matter (PM2.5 or PM10), sulfur dioxide (SO₂), carbon monoxide (CO), nitrogen dioxide (NO₂) and ozone (O₃). See Appendix A.1 for descriptive statistics. The EPA provides further details on AQI calculation in EPA (2018).

¹³We calculate wind speed for our control variables as $WSPEED_i = \sqrt{u_i^2 + v_i^2}$.

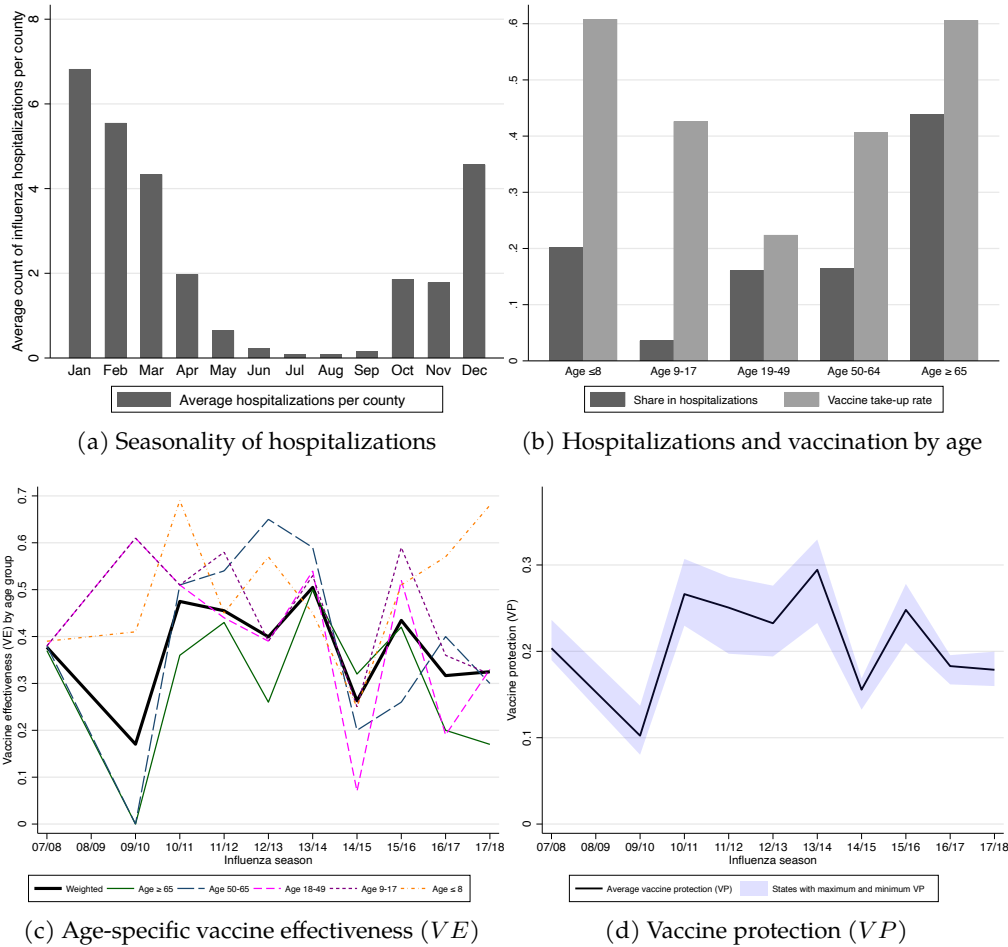


Figure 1: Descriptive figures on influenza inpatient hospitalizations and vaccine take-up and effectiveness

Notes: Panel (a) shows the average count of influenza inpatient hospitalizations per county-month in the [HCUP \(2018b\)](#) data. Panel (b) shows the age group shares of influenza inpatient admissions, as well as age group-specific vaccine take-up, both pooled across states and time. Panel (c) plots (raw) reported vaccine effectiveness for each age group over influenza seasons (with the exception of 08/09 where no data are available). The thick black line plots our weighted measure of overall vaccine effectiveness. Panel (c) plots vaccine protection averaged across states as the thick line. The bands illustrate the variation within each season across states by plotting the states with the maximum and minimum vaccine protection in each season.

by age group and Figure A.4b by race. Figure A.4c shows spatial variation by taking a cross-section of vaccine take-up rates among those 65 years and older across different states in a given influenza season, in this case 2009/2010. The figures illustrate that the variation in vaccine take-up is larger across age groups than across racial groups, across time or across space.

We obtain measures of vaccine effectiveness by influenza season and age group, VE^{raw} , from the studies underlying CDC estimates ([CDC 2019](#)), available beginning in the 2007/2008 season ([Belongia et al. 2011](#), [Griffin et al. 2011](#), [Treanor et al. 2012](#), [Ohmit et al. 2014](#), [McLean et al. 2015](#), [Gagliani et al. 2016](#), [Zimmerman et al. 2016](#), [Jackson et al. 2017](#), [Flannery et al. 2019](#), [Rolfes et al. 2019](#), [Flannery et al.](#)

2020) with the exception of the 2008/2009 season.¹⁴ These studies measure vaccine effectiveness as the vaccination-induced percentage reduction in the odds of testing positive for influenza conditional on having influenza-like symptoms. One can interpret vaccine effectiveness as the approximate share of vaccinated people who do not test positive but would have absent the vaccine.¹⁵

Figure 1c plots age-specific vaccine effectiveness against influenza season, showing variation both across seasons and age groups. Across seasons, the match between circulating viral strains and the vaccines based on forecasts is imperfect and varies due to antigenic drift. Within a season, the match can be of different quality for different age groups due to “original antigenic sin” (Francis 1960); the first influenza strain to which the immune system is exposed imprints immunological memory with that specific strain, such that different generations with different antigenic imprints respond differently to new vaccines and strains within years.

Constructing vaccine protection: The share of people protected by the vaccine in each season and state is a combination of take-up rate VR and age group-weighted vaccine effectiveness VE . As an example, for a group with homogeneous effects from exposure, if 50% of people are vaccinated, but the vaccine is only 30% effective, the effective vaccine protection (VP) is the same as when only 30% of people are vaccinated but the vaccine is 50% effective. For groups with heterogeneous vulnerability, aggregate hospitalizations also depend on whether those individuals that are more vulnerable than others have a higher take-up rate or vaccine effectiveness. An 80-year old without a vaccine, for example, is much more likely to be hospitalized with influenza than a 30-year old without a vaccine. Figure 1b shows hospitalization incidence is highest for two age groups: 65-years and older and 8-years and younger.¹⁶ To construct a population-level measure of vaccine protection that accounts for such differences in vulnerability, we weight age-specific vaccine take-up rates and vaccine effectiveness by influenza hospitalization shares of each age group:

$$VP_{cs} = \frac{1}{\sum_a (\overline{HS}_a)} \sum_a VE_{sa}^{raw} \times VR_{csa} \times \overline{HS}_a \quad (1)$$

where c denotes counties (VR_{csa} varies at the state level, but we index by counties for simpler notation in the following sections), s denotes influenza seasons, and a denotes age groups. Hospitalization weights \overline{HS}_a are a simple average across influenza seasons s , i.e., $\overline{HS}_a = \frac{1}{S} \sum_s HS_{sa}$, and the first term $\frac{1}{\sum_a (\overline{HS}_a)}$ ensures that the age weights sum to one, such that overall hospitalizations do not affect our values of VP_{cs} . We plot VP_{cs} averaged across states in Figure 1d, along with the VP_{cs} of the state with

¹⁴The CDC measures vaccine effectiveness across influenza seasons rather than calendar years, as seasons overlap calendar years (e.g., October-December for year y and January-March for year $y + 1$).

¹⁵The odds ratio is approximately the relative risk due to a small number of influenza positive cases (Zhang & Kai 1998).

¹⁶We construct groups with these age cutoffs because they coincide with the common age cutoffs in vaccine effectiveness studies.

the highest and lowest VP_{cs} in each influenza season. The minimum of VP_{cs} is 0.08 and the maximum is 0.33.

Since VP is constant within the season, vaccination rates VR_{csa} that differ across states solely drive cross-sectional spatial variation in VP_{cs} . The sources of temporal variation in VP_{cs} are both vaccination rates VR_{csa} and vaccine effectiveness VE_{sa}^{raw} which vary across influenza seasons. Equation (1) shows that a 10% increase in VP_{cs} can either be the result of a 10% increase in vaccine rates in all age groups or a 10% increase in vaccine effectiveness in all age groups (or some combination of both effects). For our analysis of heterogeneity across different age groups, we only use vaccination rates and vaccine effectiveness for the relevant age groups in constructing VP_{cs} . For heterogeneity analysis across different racial groups, we use our overall measure of vaccine protection scaled by the ratio of race specific take-up in a season to overall vaccine take-up in a season.

Mortality and emergency department (ED) visits: Although our primary focus is on inpatient hospitalizations, we also extend our analysis to consider influenza-related emergency department visits and mortality. Data on visits to emergency departments is from [HCUP \(2018a\)](#), and has overlapping spatial coverage with our main inpatient data. Individual level mortality data from [NCHS \(2019\)](#) covers every county in the U.S. and includes deaths that happen inside or outside of hospitals. For both ED visits and mortality, we count every hospitalization or death with influenza as primary cause as above, and aggregate to the county-by-year-by-month level.

Socio-demographics: We use employment counts at the county-by-year-by-month level from the [of Labor Statistics \(2021\)](#) as an additional control in robustness checks. Our analysis of policy implications utilizes county population data by race from the 2010 U.S. Census and county median income data from [Chetty et al. \(2018\)](#).

II. Empirical Strategy

Given the nature of our outcome variables, we estimate count models as our primary specification, though we also estimate linear models as a specification check. We estimate the relationship between the count of influenza-related inpatient hospitalizations H_{cym} and the lagged air quality index AQI_{cym-1} at the county c by year y by calendar month m level using the following conditional exponential mean function (consistent with a Poisson count data model):

$$E[H_{cym}|AQI_{cym-1}, \mathbf{X}_{cym}, \gamma_{csy}, \mu_{ym}] = \exp(\beta AQI_{cym-1} + \mathbf{X}'_{cym} \delta_1 + \mathbf{X}'_{cym-1} \delta_2 + \gamma_{csy} + \mu_{ym}). \quad (2)$$

We lag the AQI one month to capture exposure to air pollution before hospital admission, and control for a wide variety of both regional and temporal factors. Our preferred specification includes county-

by-season-by-year (γ_{csy}) and year-by-month fixed effects (μ_{ym}). Since each influenza season s spans October through March and overlaps calendar years y and $y + 1$, the county-by-season-by-year fixed effects (γ_{csy}) are tantamount to county-by-quarter-by-year fixed effects.¹⁷ While county-by-quarter-by-year fixed effects capture the bulk of climatic differences across counties, we also include contemporaneous weather controls X_{cym} and lagged weather controls X_{cym-1} to address the link between both influenza and weather (temperature and humidity can influence influenza transmission rates) and weather and pollution (different climatic conditions can lead to different levels of air quality) within county-quarter-years.¹⁸ Note that our outcome variable is the count of influenza hospitalizations, but inclusion of our fixed effects in Equation (2) ensures our estimates are equivalent to recovering the effect on hospitalization *rates* per capita.¹⁹

County-by-season-by-year (or county-by-quarter-by-year) effects γ_{csy} control for differences in unobserved confounders that influence pollution exposure and health outcomes across counties separately for every quarter-by-year, such as demographics, socio-economic factors, or health care access and protocols. This also addresses a possible concern due to potential variation in random diagnostic influenza testing in hospitals that could mask true influenza rates. Our fixed effects absorb potential bias from discrepancy between actual and observed hospitalizations as long as the ratio between them is constant within county-quarter-years and/or year-months.²⁰ Year-by-month fixed effects control for seasonality and general monthly trends within each year in both influenza and pollution. For example, two common lung irritants included in the AQI, particulate matter and carbon monoxide, peak in winter months much like influenza admissions; year-by-month fixed effects capture such seasonality. In robustness checks, we examine models using alternative fixed effects specifications.

Given the included fixed effects, two remaining threats to identification are unobserved confounding within each county-by-quarter-by-year cell and measurement error in pollution assignment. For example, increased economic activity and interaction between people at the local level could drive both air pollution and influenza infections. We control for lagged employment at the county-by-year-by-month

¹⁷The county-by-season-by-year fixed effects (γ_{csy}) are equivalent to including county-by-year and county-by-season fixed effects separately.

¹⁸This includes information on temperature, specific humidity, precipitation, and wind speed. Temperature and humidity have been shown to affect both virus survival (Lowen et al. 2007, Shaman & Kohn 2009, Shaman et al. 2010, Casanova et al. 2010, Harper 1961) and air pollution (Ijaz et al. 1985, Lou et al. 2017, Greenburg et al. 1967). In our baseline model we include five quintile bins for temperature (C), five quintile bins of specific humidity, and linear terms for precipitation and wind speed, all of which include contemporaneous and lagged versions.

¹⁹Influenza hospitalizations rates H_{cym}^{rates} and counts H_{cym} relate in the following way: $H_{cym}^{rates} = H_{cym}/Pop_{csy}$, where Pop_{csy} is county population in each county-season-year cell. We can multiply both sides of Equation (2) by $\exp(\log(1/Pop_{csy}))$ such that our estimation recovers the effect on H_{cym}^{rates} as dependent variable, and the fixed effects absorb $\exp(\log(1/Pop_{csy}))$.

²⁰Suppose actual (unobserved) influenza hospitalizations H_{cym}^{actual} and measured diagnosed influenza hospitalizations H_{cym} relate in the following way: $H_{cym}^{actual} = H_{cym} \times R_{csy} \times R_{ym}$, where $R_{csy} \times R_{ym}$ captures arbitrary discrepancy between actual and observed hospitalizations. If we insert this relationship in Equation (2), we can multiply both sides by $\exp(\log(R_{csy}) + \log(R_{ym}))$ such that our estimation recovers the effect on the unobserved H_{cym}^{actual} as dependent variable, and the fixed effects absorb $\exp(\log(R_{csy}) + \log(R_{ym}))$.

level in our regressions as one approach, but this may not fully capture this relationship. Measurement error may arise because of the sparse nature of pollution monitors. To address these issues, our main strategy is to employ instrumental variables for air quality.

A. Instrumenting for air quality

We take an approach conceptually akin to that of [Deryugina et al. \(2019\)](#) by exploiting changes in wind direction as an instrument for the AQI. The idea behind the instrument is that wind blowing from a particular direction moves around the pollution internal to the county but also brings in external pollution. Appendix Figure A.5 provides an illustration using Suffolk County, which contains the city of Boston, as an example. The polar plot indicates that monthly AQI is much higher when prevailing winds are blowing from the South-West, which is the direction of major polluting sources along the eastern seaboard. The AQI is, however, much lower when prevailing winds are blowing from the East, which brings in cleaner air from the ocean. Recall, however, that we are not using these values as our instrument for air pollution, as individuals may sort based on prevailing wind patterns. Instead, we use monthly *changes* in wind directions as our source of variation that shifts pollution, net of average pollution in the county. For example, if prevailing winds change from South-West to East in Boston, our instrument would shift pollution down for that particular month, net of average pollution levels in Boston in that year-quarter, conditional on our fixed effects and controls. The identifying assumption is that, conditional on our weather controls and fixed effects, wind direction affects influenza hospitalizations only through its effect on the AQI, but does not have a direct effect on hospitalizations. Those exogenously determined changes in wind direction (conditional on wind speed, other weather controls and the various fixed effects) result in changes in pollution levels in a neighborhood that are likely to be uncorrelated with local determinants of pollution.

While we borrow the premise of this design from [Deryugina et al. \(2019\)](#), we modify the precise construction of the instruments. Specifically, [Deryugina et al. \(2019\)](#) construct instruments (Z_i^D) by using dummy variables for wind direction bins $WDIR_i^q$ (e.g., $WDIR_i^{NW}$ for when wind is blowing from the North-West for observation i belonging to a particular county in a particular point in time) interacted with geographical region level indicators G_c : $Z_i^D = \sum_c \sum_q WDIR_i^q \times G_c$. One challenge in constructing this set of instruments is the choice of geographical granularity for G_c . On the one hand, if G_c are large regions including multiple counties, a particular wind direction requires that pollution shifts in the same direction and to the same degree for all counties in the same group G_c . Counties just North or just South of an urban center, however, are likely to receive the pollution shock when wind blows from the opposite direction, rather than from the same direction. Similarly, a county South of a large urban center, and a county South of a small urban center, should receive a pollution shock when wind is blowing from the North, but the size of the pollution shock likely differs. On the other hand,

if G_c are small entities, e.g., counties themselves, each county is allowed to have different pollution shocks in different sizes from different wind directions, but the set of instruments grows larger than the number of panels or counties N_c . This can lead to computational difficulties and inefficient standard errors.²¹ [Deryugina et al. \(2019\)](#) balance this trade-off by selecting the granularity of G_c based on a k -means cluster algorithm, which generates groups that include nine counties on average.

We instead solve this trade-off by using a different approach that allows full flexibility in how wind directions shift pollution in different counties (i.e., G_c at the county level), while dramatically reducing the number of instruments as well. Instead of interacting wind direction bins with county indicators, we transform the values in the wind direction dummies to capture both the sign and size of pollution shocks from changes in wind direction for each county. We do this in two steps. First, we create a new variable $A\tilde{Q}I^{qc}$ which is pollution in county c averaged over the entire sample when wind is blowing from direction q in county c , demeaned by the average pollution level in county c :

$$A\tilde{Q}I^{qc} = \frac{1}{\sum_{i \in q_c} \sum_{i \in q_c} A Q I_i^{qc}} - \frac{1}{\sum_{i \in c} \sum_{i \in c} A Q I_i} \quad (3)$$

We then use $A\tilde{Q}I^{qc}$ to generate a set of instruments Z_i^q , where each instrument corresponds to a particular wind direction (e.g., Z_i^{NW}), and the values of Z_i^q are populated by $A\tilde{Q}I^{qc}$ if a particular observation i belongs to county c and the wind in this particular year-month in this county is blowing from q :

$$Z_i^q = \begin{cases} A\tilde{Q}I^{qc} & \text{if } WDIR_i^q = q \text{ and } i \in c, \\ 0 & \text{otherwise} \end{cases} \quad (4)$$

This generates N_q instruments instead of $N_q \times N_c$ instruments. Z_i^q also addresses the two restrictions that arise when pooling multiple counties into groups. First, a single coefficient on a particular wind direction bin (e.g., the coefficient for Z_i^{NW}) accounts for different signs of pollution shocks for different counties from the same wind direction. For example, a county South-East of a major urban center is likely to have a positive value in Z_i^{NW} , whereas a county North-West of the major urban center is likely to have a negative value in Z_i^{NW} . Therefore the coefficient for Z_i^{NW} can shift pollution for the two counties into different directions. Second, a single coefficient on a particular wind direction bin also accounts for different sizes of pollution shocks. For example, a county South-East of a large urban center may experience larger pollution shocks when wind blows from the North-West than a county

²¹Optimal (two-step) GMM with a clustered weighting matrix at the county level is infeasible, for example, because the number of instruments is larger than the number of clusters.

South-East of a small urban center. Since the average size of pollution shocks is captured in Z_i^{NW} , the same coefficient on Z_i^{NW} can shift pollution to a different extent in different counties.

We design the instruments Z_i^q to capture pollution shocks that occur from changes in wind direction. Since we use wind-induced pollution shocks averaged across the entire sample when constructing Z_i^q , we do not capture individual events that generate pollution shocks that only occur in a particular year-month in a particular county, which could be problematic since they may also correlate with influenza cases.²² We also control for changes in weather that might affect influenza hospitalizations directly and correlate with changes in wind direction, such as temperature, humidity, precipitation or wind speed. Finally, since we use a one-month lagged AQI as our variable of interest, we use a one-month lagged wind direction instrument to form our moment conditions.

For our baseline model, we use the four quadrants as wind direction bins, but have also performed robustness checks with alternative numbers of wind direction bins. We estimate our instrumented model with a Poisson GMM-IV procedure that accounts for fixed effects through quasi-mean differencing, and construct moment conditions with our set of instruments. Note that the non-instrumented Poisson GMM estimates are numerically equivalent to a Poisson Pseudo-Maximum Likelihood (PPML) estimator.²³ We cluster standard errors at the county level to allow for arbitrary heteroskedasticity and serial correlation. For our linear specification, we use the corresponding Linear GMM-IV procedure that is numerically equivalent to standard linear GMM optimization. We provide econometric details in Appendix A.2.

As an expansion, we include further instruments for AQI based on thermal inversions (Arceo, Hanna & Oliva 2016). Typically, air is colder the farther from the earth's surface. Thermal inversions appear when a warm air layer moves above a cold air layer, reducing air cycling and generating stagnant air conditions. While inversions do not directly affect health (conditional on temperature), they trap pollutants closer to the ground, leading to increases in pollution concentrations.²⁴ We use the share of days with inversions and the average strength of inversions at the county-year-month level. We then interact both variables with a scaling variable that is the average county AQI across the entire sample. This allows inversions in more pollution-intensive regions (e.g., large urban centers) to shift pollution more than in less pollution-intensive regions (e.g., rural counties).

While our Poisson GMM-IV fixed effects estimation does not have an explicit first stage regression as in two-stage least squares estimations, we can approximate a first stage by running a linear regression

²²Identification does not use prevailing wind direction, which would not change across time and, as Deryugina et al. (2019) note, could lead to sorting or strategic placement of pollution monitors. Instead, our instrument uses month-to-month changes in wind patterns in a given county by year by quarter cell, which should not affect sorting or monitor placement.

²³We show the PPML (Correia, Guimarães & Zylkin 2019) estimates in the Appendix. The PPML point estimates are consistent as long as the conditional mean is correctly specified, irrespective of the distribution of the outcome or errors (Gourieroux et al. 1984). The PPML estimator performs well with a large number of zeros and over- or under-dispersion in the data (Silva & Tenreiro 2006, 2011).

²⁴We use inversions between midnight and 6AM to limit potential confounding through behavioral responses.

of AQI on our instruments and controls. Table A.3 in Appendix A.3 shows that our wind instruments shift pollution with a Kleibergen-Paap F-stat of 176.8 (Column (1)).²⁵ Inversions also shift pollution, however, the Kleibergen-Paap F-stat is lower at 8.6 when including inversions alone (Column (4)), and 91 when including wind direction and inversion instruments simultaneously (Column (7)).²⁶ For this reason, our preferred specification relies solely on the instruments based on wind direction, though we also show results with both sets of instruments.

B. Vaccines

To estimate the impact of vaccine protection (VP_{cs}) on the pollution-hospitalization relationship, we modify Equation 1 to include an interaction term $AQI_{cym-1} \times VP_{cs}$, noting that the base effect VP_{cs} is absorbed in the fixed effects γ_{csy} :

$$\begin{aligned} E[H_{cym} | AQI_{cym-1}, VP_{cs}, \mathbf{X}_{cym}, \gamma_{csy}, \mu_{ym}] \\ = \exp(\beta_1 AQI_{cym-1} + \beta_2 (AQI_{cym-1} \times VP_{cs}) + \mathbf{X}'_{cym} \boldsymbol{\delta}_1 + \mathbf{X}'_{cym-1} \boldsymbol{\delta}_2 + \gamma_{csy} + \mu_{ym}) \end{aligned} \quad (5)$$

Several econometric challenges exist in evaluating how the influenza vaccine alters the effect of pollution on influenza. Recall vaccine protection VP_{cs} is a composite measure of vaccine take-up and effectiveness. Individuals may reduce avoidance behavior if vaccinated, or be more likely to get the vaccine in seasons with more reported influenza cases, both of which attenuate the raw effect of the vaccine. Selection bias in vaccine take-up may also pose a problem if the most susceptible or most cautious are more likely to seek out vaccines. To address these issues, we instrument for potentially endogenous vaccine protection (VP_{cs}) using exogenous vaccine effectiveness (VE_s). Our identifying variation exploits the natural variation in vaccine effectiveness, determined by the random variations in the quality of the match between the influenza vaccine and the viral strain in circulation.²⁷ Note that at the time of vaccination, which is usually early in the influenza season, it is not yet known how effective the vaccine will turn out over the course of the season. Therefore, vaccine take-up should generally not be affected by vaccine effectiveness. We confirm this empirically by regressing take-up on effectiveness separately for our five age groups and find no statistically significant association in any of the five regressions.

²⁵Note that all wind direction bins have a positive coefficient, because the values of the instrument are negative when a particular wind direction tends to blow in clean air for a particular county. The coefficients should converge to one as the sample size grows, either through the number of years or number of counties. Table A.4 shows this pattern in a Monte Carlo simulation of the approximated first stage regression.

²⁶Note that the sum of the two coefficients, the coefficient on the interaction between share of inversion days with the county average AQI (\overline{AQI}) and the coefficient on share of inversion days, is positive at the average of \overline{AQI} (34.7), and the same holds for the strength of inversions.

²⁷See also Ward (2014) and White (2019) who, however, calculate vaccine effectiveness based on the names of the viral strains in the vaccine and in circulation, which in contrast to our measure, do not take into account variations in vaccine effectiveness across age groups and imperfectly map into clinical measures of effectiveness.

Effectiveness based on antigenic drift is, in principle, orthogonal to unobserved determinants of health in a given year. This provides insights into how vaccines affect the pollution-induced spread of influenza and provides a test of the causal effects of pollution on influenza. If vaccines moderate the effect of pollution on influenza, it must be that pollution causally relates to influenza hospitalizations, though we cannot distinguish between whether the vaccine is: (i) reducing the probability any pollution-harmed individual is exposed to the flu due to external benefits from vaccination of others, or (ii) changing the probability that a pollution-harmed individual contracts a severe case of flu when exposed.

To generate an overall measure of vaccine effectiveness (VE_s) to instrument for VP_{cs} , we construct a weighted average of time-varying age specific raw vaccine effectiveness (VE_{sa}^{raw} , which Figure 1c shows). The weights for age groups are time-invariant and capture the age groups where vaccine effectiveness matters relatively more: those with a greater tendency of hospitalization and those with higher vaccine take-up rates. Figure 1b shows these weights and that both hospitalization incidence and vaccination rates are highest for those 65-years and older and 8-years and younger, the two most vulnerable groups in our sample. Our measure of vaccine effectiveness is:

$$VE_s = \frac{1}{\sum_a (\overline{VR}_a \times \overline{HS}_a)} \sum_a VE_{sa}^{raw} \times \overline{VR}_a \times \overline{HS}_a, \quad (6)$$

where vaccine take-up rate weights \overline{VR}_a and hospitalization shares \overline{HS}_a are simple averages across influenza seasons s , e.g. $\overline{VR}_a = \frac{1}{S} \sum_s VR_{sa}$, and the first term $\frac{1}{\sum_a (\overline{VR}_a \times \overline{HS}_a)}$ ensures that the age weights sum to one such that overall vaccine take-up or hospitalizations do not affect our values of vaccine effectiveness. As we use time-averaged hospitalization shares and vaccination rates, vaccine effectiveness is the only source of temporal variation in our instrument.²⁸ Figure 1c shows our final measure of weighted vaccine effectiveness ranges between 0.17 and 0.51 during our study period.

By defining vaccine protection as a combination of vaccine effectiveness and vaccine take-up, we interpret β_2 as a change in either component, suggesting policy can focus on either measure. This helps maintain a direct policy implication of our results — while random variation in vaccine effectiveness provides a compelling identification strategy, policy efforts to improve it are met with limited success. Vaccine take-up rates, however, may be more amenable to policy intervention through efforts to reduce the costs of obtaining a vaccine or promote its benefits. With this policy lens in mind, we discuss changes in β_2 as the effect of a relative increase in vaccine take-up rates.

²⁸A potential threat to the exclusion criteria for our instrument occurs if shocks that increase the spread of influenza (e.g., a sporting event associated with a local team as in [Stoecker, Sanders & Barreca \(2016\)](#)), also increase influenza mutation rates and thus weaken vaccine effectiveness. This concern is likely limited, as recent research suggests that random mutations during vaccine production, not from virus spread itself, drives mismatch of vaccines and strains in circulation. For discussion of this research, see ([Cohen 2017](#)).

Table 1: The effect of air pollution on severe influenza cases

	Influenza is primary ICD code				Influenza is any ICD code				Influenza is only ICD code			
	Poisson GMM (1)	Poisson GMM (2)	Poisson GMM-IV (3)	Poisson GMM-IV (4)	Poisson GMM (5)	Poisson GMM (6)	Poisson GMM-IV (7)	Poisson GMM-IV (8)	Poisson GMM (9)	Poisson GMM (10)	Poisson GMM-IV (11)	Poisson GMM-IV (12)
AQI	.0076 (.0024)	.034 (.0076)	.028 (.0074)	.11 (.026)	.0082 (.0024)	.031 (.007)	.021 (.0069)	.088 (.024)	.014 (.0058)	.037 (.02)	.043 (.017)	.11 (.049)
AQI X VP		-.14 (.036)		-.53 (.16)		-.12 (.032)		-.41 (.14)		-.13 (.1)		-.49 (.32)
Observations	17668	17668	17668	17668	20013	20013	20013	20013	3954	3954	3954	3954
Mean of outcome	6.04	6.04	6.04	6.04	11.05	11.05	11.05	11.05	0.81	0.81	0.81	0.81
Mean of AQI	35.27	35.27	35.27	35.27	35.06	35.06	35.06	35.06	38.07	38.07	38.07	38.07
Mean of VP	-	0.21	-	0.21	-	0.21	-	0.21	-	0.2	-	0.2
Mean of VE	-	0.36	-	0.36	-	0.36	-	0.36	-	0.35	-	0.35

Notes: The dependent variable in Columns (1-4) is the count of inpatient hospital admissions with influenza as primary diagnosis within a county-year-month. The dependent variable in Columns (5-8) is the count of inpatient hospital admissions with influenza as any (primary or secondary) diagnosis within a county-year-month. The dependent variable in Columns (9-12) is the count of inpatient hospital admissions with influenza as only diagnosis within a county-year-month. We limit analysis to the influenza intensive months of October through March and our sample spans 2007-2017 with the exception of October 2008 to March 2009 where vaccine effectiveness data is not available. Vaccine protection (VP) is weighted by hospitalization shares across age groups and is measured between 0 (low) and 1 (high). The results are from a Poisson GMM estimation with county-by-season-by-year fixed effects and year-by-month dummies as well as weather controls. Weather controls consist of five bins of temperature quintiles, five bins of specific humidity quintiles, and linear terms for precipitation and wind speed. All weather variables are based on county-year-month averages. The air quality index (AQI) is lagged one month and a higher AQI means worse air quality. The columns indicating “GMM-IV” use our instruments based on wind direction instead of the AQI to generate moment conditions, and in even-numbered columns additionally use our VE instrument instead of VP to form moment conditions. The number of included observations can vary across different outcomes due to fixed effects and varied counts in each county-year-month cell. Standard errors in parentheses are clustered at the county level.

To estimate Equation (5), we use the same Poisson GMM-IV fixed effects estimator as for Equation (2) with wind direction instruments for the AQI. The moment conditions for our interaction term $AQI \times VP$ use the interaction of wind direction instruments with our VE instrument. Table A.3 in Appendix A.3 shows that our wind instruments interacted with VE shift the interaction term with a Kleibergen-Paap F-stat of 35.3 (Column (3)).

III. Results and Discussion

A. Influenza Hospitalizations

Table 1 shows estimates from our Poisson GMM estimations. Coefficients represent the AQI semi-elasticity of the count of inpatient hospitalizations with primary diagnosis influenza within a county-year-month, or an approximate percentage change in inpatient counts per unit of AQI when estimates are sufficiently small. Estimates from Column (1) correspond to Equation 2, without using any instruments, and imply a 1-unit increase in the monthly AQI associates with a 0.76% increase in influenza inpatient admissions. Column (3) shows that the estimate is larger when using instruments for the AQI based on wind direction. Given that the non-instrumented estimates contain county-by-quarter-by-year fixed effects, they likely control for many potential sources of confounding, such as residential sorting or economic activity. Much of the remaining bias in the non-instrumented estimates is likely due to measurement error. If this error is classical, estimates will be biased to the null, and the IV approach will generate larger (absolute) estimates. Our larger IV estimates are consistent with this, as well as the

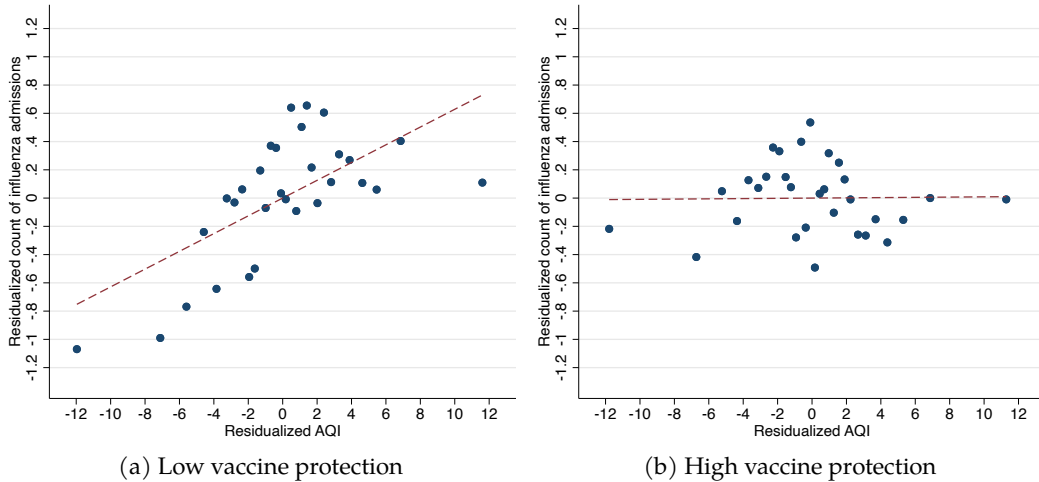


Figure 2: Air quality and vaccine protection

Notes: Panels (a) and (b) show binned scatterplots with 30 bins and a linear regression on the underlying data. Each shows the correlation net of county-by-season-by-year and month fixed effects as well as weather controls, where the vertical axis shows the residuals from a Poisson regression and the horizontal axis the residuals from a linear regression without instruments. The panels show the relationship for below (a) and above (b) median vaccine protection in the sample.

patterns found in [Deryugina et al. \(2019\)](#).²⁹ Specifically, our IV approach finds that a 1-unit increase in the monthly AQI results in a 2.8% increase in influenza inpatient admissions. To put this estimate into a national context, a one-standard-deviation increase in AQI (10.9-unit increase in our data) amounts to approximately 27,182 (35.7%) additional inpatient hospitalizations for a 6-month influenza season in the U.S.³⁰

To explore the moderating role of the influenza vaccine, Figure 2 shows the regression-adjusted relationship between AQI and influenza admissions separately in a sample with low vaccine protection in Panel (a) and high vaccine protection in Panel (b). We determine each group using a median vaccine protection (0.21) sample split. The relationship between air quality and admissions rates is positively sloped in Panel (a), indicating that the AQI affects flu admissions when the vaccine is a bad strain match and/or vaccine take-up is low. When vaccine protection is high, however, this relationship flattens almost completely, as Panel (b) shows, suggesting an effective vaccine with sufficient take-up nullifies the relationship between pollution and the flu. This does not imply a high vaccine protection eliminates all influenza hospitalizations or all pollution-related respiratory hospitalizations. Rather, sufficiently

²⁹The p-value of Hansen's J-statistic of overidentifying restrictions in Column (3) is 0.53, so we cannot reject validity of the model.

³⁰We use the 10.9-unit increase and the coefficient 0.028 for the relative increase $\exp(0.028 * 10.9) - 1 = 0.3569$, and multiply it by the average inpatient admissions per county-year-month (4.04), the total number of US county equivalents according to the US Census Bureau (3142) ([United States Census Bureau 2018](#)) and by the 6 months within a influenza season. Note that we are using average admissions across our pre-estimation sample of summary statistics from Table A.2 (4.04), which is lower than the average reported in the estimation sample in Table 1 (6.04), since a count model drops counties with zero valued outcomes within the level of the fixed effect. This only counts cases with primary diagnosis influenza, making this estimate of absolute numbers a lower bound. Using hospitalization with any influenza diagnosis (Column (7)) doubles the additional predicted cases because the base of hospital admissions is much larger.

high vaccine effectiveness and take-up eliminate those flu hospitalizations directly attributable to the negative shock of pollution.

To test for the moderating role of vaccine protection, we present estimates of Equation (5) using our Poisson GMM framework in Table 1. Column (2) shows the estimates without using instruments, and Column (4) uses our instruments based on wind direction for the AQI, and our vaccine effectiveness instrument (VE) interacted with the wind direction instruments for the interaction term of AQI and vaccine protection (VP). The instrumented estimates are larger than the non-instrumented estimates by around the same factor as for the non-interacted results in Column (1) and (3). Vaccine protection substantially moderates pollution-driven influenza cases. Our negative interaction coefficient in Column (4) implies that a vaccine protection of 21%, which coincides with the average vaccine protection in our sample (the maximum is 33%), nullifies the link between air pollution and influenza hospitalizations. This supports prior evidence of thresholds in influenza vaccination where the positive external benefits are large enough to almost eliminate influenza spread even at incomplete vaccination take-up and effectiveness (Boulier, Datta & Goldfarb 2007, Ward 2014). In seasons with poor viral match of the vaccine (see Figure 1c), vaccine protection is substantially lower (see Figure 1d). To compensate for a drop in vaccine effectiveness from the median (0.39) to the 25th percentile (0.32), vaccine take-up would need to increase by 18% across all age groups. Table A.5 in Appendix A.3 provides reduced form results where we include vaccine effectiveness directly instead of instrumenting for vaccine protection.

In our baseline specifications in Columns (1) through (4), we include only cases where the *primary* diagnosis is influenza, thus ignoring occurrences of influenza in secondary diagnoses. This likely misses some influenza-related hospitalizations, but is arguably more robust to over-counting cases that might arise by including patients who suffer from different health conditions triggered by air pollution (e.g., asthma) and then happen to be tested for influenza upon hospital admission due to health protocols. To show robustness to different counting strategies, Columns (5) to (8) repeat our analysis counting patients that have any (primary or secondary) influenza diagnosis. This yields an average number of influenza admissions per county-year-month in our estimation sample that is roughly double (11.05) compared to our baseline approach (6.04). The estimated coefficients, which again reflect semi-elasticities, are close to baseline results both for the level effect of AQI as well as the interaction with vaccine effectiveness. In Columns (9) to (12), we use a more restrictive condition by counting hospital admissions where the only diagnosis is influenza. This reduces the average count of admissions per county-year-month to 0.81 (the majority of influenza hospital admissions have further influenza-induced complications, e.g., pneumonia). The estimated coefficients are again comparable to our baseline estimates, though with larger standard errors given the considerable drop in sample size due to more cells with zero counts.

Table 2 explores heterogeneity by age and race using our Poisson GMM-IV specifications (we show

Table 2: Heterogeneity by age and race

	$\leq 8y$		9-64y		$\geq 65y$		Black/Hispanic		White	
	(1)	(2)	(3)	(4)	(5)	(6)	(7)	(8)	(9)	(10)
AQI	.034 (.0093)	.13 (.051)	.032 (.008)	-.039 (.054)	.005 (.013)	.037 (.014)	.024 (.012)	.086 (.035)	.04 (.007)	.13 (.023)
AQI X VP		-.34 (.16)		.45 (.34)		-.33 (.15)		-.43 (.2)		-.56 (.13)
Observations	10593	10593	13984	13984	13619	13619	7740	7740	15553	15553
Mean of outcome	1.89	1.89	2.76	2.76	3.51	3.51	3.27	3.27	4.17	4.17
Mean of AQI	36.51	36.51	35.7	35.7	35.5	35.5	37.5	37.5	35.46	35.46
Mean of VP	-	0.31	-	0.16	-	0.2	-	0.21	-	0.23
Mean of VE	-	0.48	-	0.4	-	0.3	-	0.36	-	0.37

Notes: The dependent variable is the count of inpatient hospital admissions with influenza as primary diagnosis within a county-year-month. The columns indicate which age or race subgroups are counted in the dependent variable. We limit analysis to the influenza intensive months of October through March and our sample spans 2007-2017 with the exception of October 2008 to March 2009 where vaccine effectiveness data is not available. Vaccine protection (VP) is weighted by hospitalization shares across age groups and is measured between 0 (low) and 1 (high). We only use the vaccine take-up rates and raw vaccine effectiveness for the age groups indicated in each column. For the results by racial groups, we use our VP scaled by the ratio of race specific to overall vaccine take-up by season. The results are from Poisson GMM-IV estimations with county-by-season-by-year fixed effects and year-by-month dummies as well as weather controls. Weather controls consist of five bins of temperature quintiles, five bins of specific humidity quintiles, and linear terms for precipitation and wind speed. All weather variables are based on county-year-month averages. The air quality index (AQI) is lagged one month and a higher AQI means worse air quality. The results use our instruments based on wind direction instead of the AQI to generate moment conditions, and in even-numbered columns additionally use our VE instrument instead of VP to form moment conditions. The number of included observations can vary across different outcomes due to fixed effects and varied counts in each county-year-month cell. Standard errors in parentheses are clustered at the county level.

non-instrumented results in Table A.6 in Appendix A.3).³¹ Columns (1) through (6) show results for three distinct age groups: up to age 8, age 9 through 64, and age of at least 65 years, where the first and last reflect the more vulnerable groups.³² Patterns across the youngest and oldest groups are similar to each other and consistent with our main results. The interaction with vaccine protection for the middle age group, however, is imprecise and positive. A positive point estimate on the interaction term implies that vaccines do not help reduce influenza hospitalizations due to air pollution, but can still reduce influenza hospitalizations not driven by air pollution. The confidence intervals are large, however, and overlap with the confidence intervals of the other age groups, so we draw little inference from this age group estimate.

Estimates are similar across racial and ethnic groups (Blacks/Hispanics and Whites in Columns (7) through (10)), with overlapping confidence intervals.³³ Combining these results with well-established racial and ethnic differences in pollution exposure (Banzhaf, Ma & Timmins 2019, Colmer et al. 2020, Currie, Voorheis & Walker 2020) may help explain the higher influenza burdens experienced by those communities (e.g. Quinn et al. 2011). As such, our results suggest that air quality control could be an additional policy lever to help reduce severe influenza cases among these vulnerable groups, particu-

³¹For our regressions with age-specific outcomes in Table 2, we only use the vaccine take-up rate and raw vaccine effectiveness data of the corresponding age groups for constructing our overall measure of vaccine protection (VP) and vaccine effectiveness (VE). We show means of VP and VE for each regression at the bottom of the table. We note that vaccines have private and external benefits, so vaccine take-up of any one group generates positive spillovers to other groups.

³²We define these age splits based on the age splits available in the vaccine effectiveness measures.

³³We adjust vaccine protection by the seasonal ratio of vaccine take-up of the particular ethnic group to overall vaccine take-up, which results in a slightly higher mean of VP for Whites, as reported in the bottom of the table.

Table 3: The effect of air pollution and vaccines on emergency department visits and mortality

	ED visits				Mortality			
	Poisson GMM (1)	Poisson GMM (2)	Poisson GMM-IV (3)	Poisson GMM-IV (4)	Poisson GMM (5)	Poisson GMM (6)	Poisson GMM-IV (7)	Poisson GMM-IV (8)
AQI	.018 (.0027)	.059 (.01)	.038 (.0071)	.11 (.019)	.011 (.0023)	.028 (.0073)	.0014 (.008)	.053 (.029)
AQI X VP		-.22 (.047)		-.43 (.11)		-.088 (.036)		-.3 (.15)
Observations	10049	10049	10049	10049	23126	23126	23126	23126
Mean of outcome	38.4	38.4	38.4	38.4	0.96	0.96	0.96	0.96
Mean of AQI	35.3	35.3	35.3	35.3	37.41	37.41	37.41	37.41
Mean of VP	-	0.21	-	0.21	-	0.2	-	0.2
Mean of VE	-	0.37	-	0.37	-	0.35	-	0.35

Notes: The dependent variable is the count of emergency department visits (in Columns (1) to (4)) or the count of deaths (in Columns (5) to (6)), all with influenza as primary diagnosis within a county-year-month. We limit analysis to the influenza intensive months of October through March and our sample spans 2007-2017 with the exception of October 2008 to March 2009 where vaccine effectiveness data is not available. Vaccine protection (VP) is weighted by hospitalization shares across age groups and is measured between 0 (low) and 1 (high). We only use the vaccine take-up rates and raw vaccine effectiveness for the age groups indicated in each column. For the results by racial groups, we use our VP scaled by the ratio of race specific to overall vaccine take-up by season. The results are from Poisson GMM-IV estimations with county-by-season-by-year fixed effects and year-by-month dummies as well as weather controls. Weather controls consist of five bins of temperature quintiles, five bins of specific humidity quintiles, and linear terms for precipitation and wind speed. All weather variables are based on county-year-month averages. The air quality index (AQI) is lagged one month and a higher AQI means worse air quality. The results are from a Poisson GMM estimation with county-by-season-by-year fixed effects and year-by-month dummies as well as weather controls. Weather controls consist of five bins of temperature quintiles, five bins of specific humidity quintiles, and linear terms for precipitation and wind speed. All weather variables are based on county-year-month averages. The air quality index (AQI) is lagged one month and a higher AQI means worse air quality. The columns indicating “GMM-IV” use our instruments based on wind direction instead of the AQI to generate moment conditions, and in even-numbered columns additionally use our VE instrument instead of VP to form moment conditions. The number of included observations can vary across different outcomes due to fixed effects and varied counts in each county-year-month cell. Standard errors in parentheses are clustered at the county level.

larly within those communities in which vaccine access is limited and reluctance to receive the vaccine is particularly high.³⁴

Although we focus primarily on inpatient hospital admissions for influenza, Table 3 shows estimates of the effect of air pollution and vaccines on two alternative outcomes: emergency department (ED) visits and mortality. ED visits may pick up less severe cases of the flu, though visiting the ED can be plagued by selection concerns since they are more likely to serve as a source of primary care for groups with limited access to health care (Finkelstein et al. 2012). Despite the fact that our data on ED visits has slightly different geographical and temporal coverage than the data for inpatient hospitalizations, the estimates are close to our main results. In Columns (5) to (8) we instead look at influenza deaths, which are less frequent than inpatient hospitalizations but also less subject to selection concerns.³⁵ The estimates for mortality also show a similar pattern to our main results. Together, these suggest that air pollution, and the protective role of vaccines, each affect a wide range of flu case severity.

In Table 4 we perform three further tests. First, Columns (1) to (4) explore robustness to functional form by using a linear mean function, closer to standard OLS, in place of the exponential mean func-

³⁴These benefits are in addition to any improvements in pollution-related health not associated with influenza. See (Deryugina et al. 2021) for a discussion of policy targeting regarding polluted areas and vulnerable people.

³⁵Since the data on mortality covers the entire U.S., these results also improve the representativeness of our main findings. The estimation sample size reported in the table is only slightly higher than for our main results because the mortality outcome has more zeros resulting in more observations being dropped by the count model.

Table 4: Linear specification, all respiratory hospitalizations, and osteoarthritis as falsification test

	Influenza hospitalizations				All respiratory hospitalizations				Osteoarthritis			
	Linear GMM		Linear GMM-IV		Linear GMM		Linear GMM-IV		Poisson GMM		Poisson GMM-IV	
	(1)	(2)	(3)	(4)	(5)	(6)	(7)	(8)	(9)	(10)	(11)	(12)
AQI	.063 (.025)	.19 (.073)	.18 (.058)	.51 (.16)	.17 (.067)	.014 (.16)	.5 (.29)	.33 (.38)	-.00054 (.00027)	.00019 (.00084)	-.0016 (.0014)	.00069 (.0029)
AQI X VP		-.61 (.28)		-1.9 (.79)		.72 (.69)		-1.3 (2.2)		-.0034 (.0041)		-.015 (.015)
Observations	17668	17668	17668	17668	24596	24596	24596	24596	24255	24255	24255	24255
Mean of outcome	6.04	6.04	6.04	6.04	141.32	141.32	141.32	141.32	43.51	43.51	43.51	43.51
Mean of AQI	35.27	35.27	35.27	35.27	34.52	34.52	34.52	34.52	34.54	34.54	34.54	34.54
Mean of VP	-	0.21	-	0.21	-	0.21	-	0.21	-	0.21	-	0.21
Mean of VE	-	0.36	-	0.36	-	0.37	-	0.37	-	0.37	-	0.37

Notes: The dependent variable is the count of inpatient hospitalizations with influenza as primary diagnosis in Columns (1) to (4), the count of inpatient hospitalizations with any respiratory primary diagnosis in Columns (5) to (8), and the count of inpatient hospitalizations with osteoarthritis as primary diagnosis, all at the county-year-month level. We limit analysis to the influenza intensive months of October through March and our sample spans 2007-2017 with the exception of October 2008 to March 2009 where vaccine effectiveness data is not available. Vaccine protection (VP) is weighted by hospitalization shares across age groups and is measured between 0 (low) and 1 (high). The results are from a Linear GMM estimation in Columns (1) to (8) and from a Poisson GMM estimation in Columns (9) to (12), all with county-by-season-by-year fixed effects and year-by-month dummies as well as weather controls. Weather controls consist of five bins of temperature quintiles, five bins of specific humidity quintiles, and linear terms for precipitation and wind speed. All weather variables are based on county-year-month averages. The air quality index (AQI) is lagged one month and a higher AQI means worse air quality. The columns indicating “GMM-IV” use our instruments based on wind direction instead of the AQI to generate moment conditions, and in even-numbered columns additionally use our VE instrument instead of VP to form moment conditions. The number of included observations can vary across different outcomes due to fixed effects and varied counts in each county-year-month cell. Standard errors in parentheses are clustered at the county level.

tion consistent with a Poisson count model. Columns (1) and (2) show a linear GMM model without instruments (OLS), for a linear version of Columns (1) and (2) of Table 1. Columns (3) and (4) show the IV as a linear version of Columns (3) and (4) of Table 1. As in our baseline Poisson GMM model, the IV estimates in Column (3) are around three times larger than those in Column (1). Since the point estimates now reflect level effects, we divide by the mean of the dependent variable to obtain percent effects that are more readily comparable to the estimates from the count model. Doing so, the linear estimate in Column (3) of 0.18 translates to a 3% effect, which is very close to the estimate of 2.8% using the count model. Vaccine protection is also comparable in magnitude. In Appendix Table A.7, we show equivalence of our Poisson GMM estimator (without instruments) with a Poisson Pseudo-Maximum Likelihood estimator, and we estimate a linear model using the inverse hyperbolic sine (IHS) of hospitalizations as our outcome. The estimates using the IHS are similar to semi-elasticities (but, unlike the log function, allow for zeros) and can therefore be more directly compared with our baseline Poisson GMM estimates. The effect of 0.02 in Column (7) in Appendix Table A.7 is close to our baseline effect of 0.028 in Table 1. Together, these results suggest that our estimates are largely insensitive to the functional form choice of our dependent variable.

Second, we ask how the effect of air pollution on influenza hospitalization compares to the effect on any respiratory hospitalization (including influenza) in Columns (5) to (8). Here we continue to use the linear models from columns (1) to (4), which has the benefit of making direct level effect comparisons, unlike the Poisson model, which provides relative percentage effects. As indicated in Table

4, the mean of hospitalizations with any respiratory hospitalization per county-year-month (141.32) is much higher than for influenza hospitalizations alone (6.04). Columns (5) and (6) show the effect on all respiratory hospitalizations without instruments and Columns (7) and (8) with instruments. The absolute effect of a one-unit increase of the AQI on influenza hospitalizations (0.18, Column (3)) is roughly one-third of the size of the effect on all respiratory hospitalizations (0.5, Column (7)).³⁶ Assuming that outside of influenza season the effect on all respiratory hospitalizations remains the same, but the effect on influenza hospitalizations drops to zero, influenza hospitalizations due to air pollution accounts for roughly 18% of all respiratory hospitalizations due to air pollution. This suggests that the increased incidence of influenza accounts for a sizeable share of the health harms from air pollution. It also implies that greater vaccine strain matches and increased take-up rates can reduce a sizeable share of hospitalizations from air pollution.

Third, as a general specification test for our model, we perform a falsification test by repeating our analysis using an outcome we do not expect to be related to pollution or vaccines. We choose to narrow our focus to osteoarthritis, which is unlikely to be related to short-term variation in pollution. Our Poisson GMM-IV results in Column (11) and Column (12) of Table 4 indicate precise zero coefficients on the effect of AQI and the interaction with vaccine protection, lending support to our model specification. As a more comprehensive test, Appendix Figures A.6, A.7 and A.8 show our Poisson GMM-IV estimates for all ICD disease groupings separately, as long as there are sufficient number of cases in those diseases.³⁷ Compared to all other disease outcomes, we find that influenza hospitalizations are most affected by the AQI. The vast majority of disease outcomes is associated with a precise zero effect, similar to osteoarthritis. There are some diagnoses where we find that AQI increases hospitalizations (Figure A.6), such as acute bronchitis, perinatal conditions (often includes respiratory conditions), or diabetes (known to increase influenza risk (Allard et al. 2010)). Adjusting for the family wise error rate for multiple hypothesis testing renders all results insignificant, except those for our influenza outcome.

As an expansion to our wind instrumental variables, we explore an additional source of variation by using inversions in Appendix Table A.8. In Columns (1) and (2) we use only inversions (without using instruments based on wind direction). The coefficients are similar as in our main results in Table 1, with overlapping confidence intervals. We next use both the inversion and wind based sets of instruments in Columns (3) and (4), again with estimates close to our main results.³⁸ These patterns lend support

³⁶This is further corroborated when comparing the effect of air pollution on influenza with all other diagnoses groupings in Appendix Figure A.6.

³⁷We focus on disease groupings that have at least half as many occurrences as influenza. This implies a threshold mean of at least 3.02 in our outcome variable, half the mean of our influenza outcome (6.04). Including additional low occurrence diseases confirms the pattern shown in the figures.

³⁸The test of overidentifying restrictions is rejected at the 5% level, both when using inversion instruments alone and when using inversions and wind instruments jointly. The test for overidentifying restrictions is passed only with instruments based on wind direction alone as in our main results. This together with the lower first stage F-stat for inversion instruments drives using solely wind direction instruments as main results.

to the validity of our model design, and demonstrate that our IV estimates are not a unique feature of our measure of wind direction in the first stage.

Finally, Table A.9 in Appendix A.3 explores further robustness of our main Poisson GMM-IV results to changes in control variables, calculation of AQI, or including off-seasonal cases. In Columns (1) and (2), we replace our county-by-season-by-year fixed effects with coarser county-by-influenza season effects. In Columns (3) and (4) we drop all weather controls. In Columns (5) and (6) we use the full controls and additionally include lagged employment at the county-year-month level to control for economic activity at our level of analysis. In Columns (7) and (8) we do not winsorize the AQI, and in Columns (9) and (10) we do not spatially interpolate the AQI. In Columns (11) and (12) we additionally include all county-year-month cells with positive influenza hospitalization cases. The estimates remain similar to our main estimates.

B. Medical Charges

Given the above effects, we calculate the additional hospital charges attributable to pollution-associated influenza to assess the costs generated by air pollution and the role of vaccine protection in mitigating those costs.³⁹ We use hospital charges as the dependent variable in Table 5, showing only results using instruments, with non-instrumented results presented in Appendix Table A.10. Column 1 indicates that a one-unit increase in the AQI corresponds to a \$US 5,049 increase in hospital charges from hospitalizations with primary diagnosis influenza. This implies that a 10% decrease in AQI (3.5 points) reduces hospitalization charges by \$US 333 million per influenza season across the entire U.S. Column 2 shows the interaction effect with vaccine protection, and Columns 3 and 4 use a Poisson model instead of a linear model. Since the effect is a relative effect in Columns 3 and 4, the estimates are reassuringly close to our estimates in Columns 3 and 4 in Table 1 where we use the count of hospitalizations as outcome.⁴⁰

We can use the results in Column 2 to further illustrate our main results in terms of additional hospital charges. When VP is high (maximum is 0.33), an increase in AQI has no noticeable impact on *flu-specific* hospitalization charges due to the protective nature of the vaccine. In contrast, when VP is low, even small changes in the AQI generate large increases in additional influenza-specific hospitalization charges. Going from an AQI of 40 to 50 (both of which are well below US regulatory standards) generates roughly 1.5 billion \$US in additional influenza inpatient hospitalization charges at a vaccine

³⁹We use deflated hospital charges with base year 2018. Hospital charges are around \$US 29 thousand per patient per influenza diagnosed inpatient hospitalization (Appendix Table A.2). Note hospital charges are distinct from hospital costs, which are notoriously difficult to ascertain because they differ significantly across institutions and units within institutions. Further, these estimates ignore indirect costs to patients, such as forgone earnings.

⁴⁰Note that we have an equally high share of zeros regardless of whether we use hospital charges or count of hospitalizations as outcome. The better fit of an exponential (Poisson) model to data with large shares of zeros may explain why the Poisson based estimates in Columns 3 and 4 are slightly more precise than those based on a linear model in Columns 1 and 2.

Table 5: Total hospitalization charges, length of stay, and charges per day

	Total charges				Length of stay in days				Charges per day			
	Linear (1)	GMM-IV (2)	Poisson (3)	GMM-IV (4)	Linear (5)	GMM-IV (6)	Poisson (7)	GMM-IV (8)	Linear (9)	GMM-IV (10)	Poisson (11)	GMM-IV (12)
AQI	5049 (1646)	10704 (4701)	.024 (.0093)	.12 (.028)	.017 (.017)	.07 (.046)	.0065 (.0077)	.058 (.021)	2227 (867)	6526 (2305)	.026 (.008)	.14 (.023)
AQI X VP		-31769 (25069)		-.63 (.18)		-.27 (.26)		-.32 (.13)		-28847 (13852)		-.74 (.13)
Observations	17754	17754	17754	17754	17783	17783	17783	17783	9689	9689	9689	9689
Mean of outcome	174095	174095	174095	174095	2.64	2.64	2.64	2.64	72119	72119	72119	72119
Mean of AQI	35.28	35.28	35.28	35.28	35.29	35.29	35.29	35.29	36.35	36.35	36.35	36.35
Mean of VP	-	0.21	-	0.21	-	0.21	-	0.21	-	0.21	-	0.21
Mean of VE	-	0.36	-	0.36	-	0.36	-	0.36	-	0.36	-	0.36

Notes: The dependent variable are hospital charges for inpatient hospitalizations with influenza as primary diagnosis, length of stay in days, or charges per day. We limit analysis to the influenza intensive months of October through March and our sample spans 2007-2017 with the exception of October 2008 to March 2009 where vaccine effectiveness data is not available. Vaccine protection (VP) is weighted by hospitalization shares across age groups and is measured between 0 (low) and 1 (high). The results are from a Linear GMM estimation and from a Poisson GMM estimation as indicated, all with county-by-season-by-year fixed effects and year-by-month dummies as well as weather controls. Weather controls consist of five bins of temperature quintiles, five bins of specific humidity quintiles, and linear terms for precipitation and wind speed. All weather variables are based on county-year-month averages. The air quality index (AQI) is lagged one month and a higher AQI means worse air quality. All results use our instruments based on wind direction instead of the AQI to generate moment conditions, and in even-numbered columns additionally use our VE instrument instead of VP to form moment conditions. Standard errors in parentheses are clustered at the county level.

protection of 0.086, the minimum in our sample.⁴¹ Conversely, when air quality is high (AQI<20), a drop in VP generates little additional pollution-driven influenza hospitalization charges (though influenza cases that are not pollution driven still might be greatly affected). On the other hand, when air quality approaches an AQI of 70 (which is still relatively clean by WHO standards), VP is highly impactful. In particular, a drop in vaccine protection from its median (0.21) to the 25th percentile (0.16), generates around 0.6 billion \$US in additional pollution-driven influenza charges when AQI is at the low end of our sample range and around 2.1 billion \$US at the high end of the pollution range.⁴²

We also decompose the effect on total charges into the effect on length of stay in days (Columns 5 to 8 of Table 5) and charges per day (Columns 9 to 12). Examining these two outcomes may also help to shed some light on whether pollution is likely to increase severity or spread of flu. Our results show a positive but statistically insignificant increase in length of stay, and a statistically significant increase in charges per day. We interpret these results as supporting the idea that pollution leads to more intense cases of the flu, i.e., it increases severity. We note, however, that we cannot properly disentangle the spread versus severity story, as we only observe the joint outcome of likelihood of hospitalization, and not the two separate components (the likelihood of catching the flu or the likelihood of hospitalization conditional on catching the flu).⁴³

A back of the envelope calculation based on realizations within our dataset may help place our estimates in a more useful context. Our results suggest that a 10% (3.5 AQI points) reduction in the

⁴¹ Calculated as $10 \cdot (10704 - 0.08 \cdot 31769) = 81,625$ \$US per county-month, multiplied by 3142 counties and 6 months.

⁴² Calculated as $20 \cdot (0.05 \cdot 31769) = 31,769$ and $70 \cdot (0.05 \cdot 31769) = 111,191$, both multiplied by 3142 counties and 6 months.

⁴³ Admitting more marginally sick people, for example, could undermine this exercise.

AQI in an historically bad vaccine effectiveness year (17% VE and 11% VP) would avert 12,607 (16.6%) hospitalizations across the U.S. or \$US 476 million in influenza medical charges. In contrast, a 10% improvement in either vaccine take-up or vaccine effectiveness from average vaccine take-up or effectiveness in a historically polluted year (38.2 AQI) would avert 26,378 (34.6%) of pollution driven influenza hospitalizations, or \$US 480 million.

C. Policy Implications

Since the marginal benefit from improving either VP or air quality decreases in the level of the other variable, vaccine and air quality policies can serve as substitutes in preventing pollution-induced influenza cases.⁴⁴ The optimal mix of those policies will depend on their relative costs on the margin as well as the ‘spillover’ impacts each may have on harms beyond influenza. It is also worth noting that these policies can operate on different time scales adding an additional dimension to the trade-offs across each policy. For example, reducing pollution emissions requires investments in capital equipment and takes considerable time, but informational approaches that promote vaccine take-up can bear fruit much more quickly. Regardless of the specifics, recognizing the interaction of these two policies broadens the toolkit to address the harms from either one of them, and thus necessarily allows one to obtain a given set of policy objectives at (weakly) lower costs.

The interaction of vaccine take-up and air quality policies also highlights new potential benefits from improved targeting of either policy. Given the seasonality of the flu, air quality policies could be time-varying.⁴⁵ Given our finding that influenza hospitalizations account for a significant share of all respiratory hospitalizations from pollution, more stringent air quality policies in influenza months may be particularly impactful.⁴⁶

Programs to promote vaccine take-up can also be targeted toward vulnerable communities based on socio-demographic risk factors. Using time-averaged data on vaccine take-up by state and race, air quality by county, and socio-demographic county characteristics on median household income and race from [Chetty et al. \(2018\)](#) and the U.S. Census, we ask what an increase of 10% in the overall vaccine take-up average (a 4.6 percentage point increase) achieves when targeted at different types of counties.⁴⁷ Specifically, we examine differences between the top and bottom 1% of U.S. counties in terms of racial

⁴⁴In the event that air quality improvements reduce the spread of the flu, the two policies may serve as complements rather than substitutes under certain conditions. For example, if the reproductive rate of flu is above 1 even with vaccine protection, but falls below 1 when combined with air quality policy, then the two policies may be complements. We thank Ben Olken for raising this point.

⁴⁵We thank Douglas Almond for raising this point.

⁴⁶Seasonal air quality policies are not without precedent. For example, the NOx cap-and-trade program in the U.S. only operates between May and September when ozone tends to be highest ([Deschenes, Greenstone & Shapiro 2017](#))

⁴⁷We calculate the average vaccine take-up by county using vaccine take-up rates by race and white, Black, Hispanic, and Asian population shares by county. Our calculations account for the joint statistical relationships between vaccine-take up, race, pollution exposure, and income.

population shares and median income, and use our estimated coefficients to compare the benefits of a 4.6 percentage point increase in vaccine take-up across these scenarios.⁴⁸

Increasing vaccine take-up in a county with high versus low Black population shares reduces hospitalizations and associated charges by 40.7% versus 26.8%. The difference is substantial, since pollution exposure is higher and vaccine take-up lower in communities with higher shares of Black residents. Interestingly, we find little difference in results when stratifying by income. Targeting a high income versus a low income county reduces pollution-induced influenza hospitalizations and associated charges by 36.4% versus 38.0%. Correlations in our data suggest that these effects are similar due to two offsetting forces. High income counties tend to include major cities, which are more polluted than more rural areas (increasing the benefits of vaccine-take up), but also have higher baseline vaccine take-up rates (decreasing the benefits). To some degree, this supports the conjecture that air quality controls and vaccine take-up can serve as substitutes.

IV. Conclusion

Using a rich, longitudinal dataset, we provide evidence that air pollution increases seasonal influenza hospitalization rates, and that improved vaccine protection, either through high vaccine effectiveness or vaccine take-up, greatly diminishes this relationship and reduces the social and medical costs of poor air quality. Our empirical strategy, based on instrumental variables using wind direction and the stochastic nature of vaccine effectiveness across influenza seasons, limits risks of confounding. Our results are robust to numerous assumptions about functional form, omitted variables, alternative outcomes, and falsification tests.

That policies to combat air quality can protect citizens from the most serious threats of influenza is a new insight that offers an additional tool in the global battle against the flu. At the same time, it appears that increased flu vaccination rates and improvements in flu vaccine strain matches can avert some of the harms from pollution. As such, the returns to policies designed to address pollution and infection externalities are inextricably connected, such that approaching either in isolation will be sub-optimal from a social welfare perspective. Thus, optimal policy strategies can help decrease medical spending, avoid lost productivity, and reduce loss of life. These returns may be particularly high in dense urban centers around the world, and developing countries in particular, where population density and high levels of pollution ([de Lataillade, Auvergne & Delannoy 2009](#)) increase the intensity of these interactions.

Our insights regarding compounding risks from pollution and flu may extend to other viral respiratory illnesses with similar etiological pathways. For example research early in the COVID-19 pan-

⁴⁸We use the median county AQI and vaccine-take up rate in the bottom and top 1% of counties.

demographic suggested significant positive correlations between COVID-19 hospitalizations and pollution levels (Wu et al. 2020).⁴⁹ While vaccine developments aid against such health threats, new strains and viruses may emerge that diminish such protection. Our results suggest an additional possible policy direction, whereby environmental controls serve as an investment to optimally manage the harms from new viral threats if effective vaccines are not available, while also providing additional protection against more established respiratory infections that may drain the healthcare system during times of crises.

REFERENCES

- Allard, Robert, Pascale Leclerc, Claude Tremblay, and Terry-Nan Tannenbaum. 2010. "Diabetes and the severity of pandemic influenza A (H1N1) infection." *Diabetes care*, 33(7): 1491–1493.
- Arceo, Eva, Rema Hanna, and Paulina Oliva. 2016. "Does the effect of pollution on infant mortality differ between developing and developed countries? Evidence from Mexico City." *The Economic Journal*, 126(591): 257–280.
- Banzhaf, Spencer, Lala Ma, and Christopher Timmins. 2019. "Environmental justice: The economics of race, place, and pollution." *Journal of Economic Perspectives*, 33(1): 185–208.
- Belongia, Edward A, Burney A Kieke, James G Donahue, Laura A Coleman, Stephanie A Irving, Jennifer K Meece, Mary Vandermause, Stephen Lindstrom, Paul Gargiullo, and David K Shay. 2011. "Influenza vaccine effectiveness in Wisconsin during the 2007–08 season: comparison of interim and final results." *Vaccine*, 29(38): 6558–6563.
- Boulier, Bryan L, Tejwant S Datta, and Robert S Goldfarb. 2007. "Vaccination externalities." *The BE Journal of Economic Analysis & Policy*, 7(1).
- Brauer, Michael, Gerard Hoek, Patricia Van Vliet, Kees Meliefste, Paul H Fischer, Alet Wijga, Laurens P Koopman, Herman J Neijens, Jorrit Gerritsen, Marjan Kerkhof, et al. 2002. "Air pollution from traffic and the development of respiratory infections and asthmatic and allergic symptoms in children." *American journal of respiratory and critical care medicine*, 166(8): 1092–1098.
- Casanova, Lisa M, Soyoung Jeon, William A Rutala, David J Weber, and Mark D Sobsey. 2010. "Effects of air temperature and relative humidity on coronavirus survival on surfaces." *Appl. Environ. Microbiol.*, 76(9): 2712–2717.
- CDC. 2008. *Behavioral Risk Factor Surveillance System (BRFSS) Survey Data 2007-08*. Centers for Disease Control and Prevention.
- CDC. 2009. *Estimated proportion of persons aged ≥6 months who received an influenza vaccination during the 2008-09 influenza season (September 2008 through February 2009), by age group, high-risk status, and race/ethnicity, National Health Interview Survey (NHIS), United States*. Centers for Disease Control and Prevention.
- CDC. 2015. *Cumulative monthly influenza vaccination coverage estimates for persons 6 months and older by State, HHS Region, and the United States, National Immunization Survey-Flu (NIS-Flu) and Behavioral Risk Factor Surveillance System (BRFSS), 2009-10 influenza season*. Centers for Disease Control and Prevention.
- CDC. 2019. *Seasonal Flu Vaccine Effectiveness Studies*. Centers for Disease Control and Prevention, National Center for Immunization and Respiratory Diseases (NCIRD).
- CDC. 2020. *Influenza vaccination coverage estimates for persons 6 months and older by state, HHS region, and the United States, National Immunization Survey-Flu (NIS-Flu) and Behavioral Risk Factor Surveillance System (BRFSS), 2010-11 through 2018-19 influenza seasons*. Centers for Disease Control and Prevention.

⁴⁹See e.g. Cui et al. (2003) for evidence on the earlier SARS-CoV.

- Chen, Pei-Shih, Feng Ta Tsai, Chien Kun Lin, Chun-Yuh Yang, Chang-Chuan Chan, Chea-Yuan Young, and Chien-Hung Lee. 2010. "Ambient influenza and avian influenza virus during dust storm days and background days." *Environmental health perspectives*, 118(9): 1211–1216.
- Chetty, Raj, John N Friedman, Nathaniel Hendren, Maggie R Jones, and Sonya R Porter. 2018. "The opportunity atlas: Mapping the childhood roots of social mobility." *NBER working paper*, , (25147).
- Cienciewicz, Jonathan, and Iona Jaspers. 2007. "Air pollution and respiratory viral infection." *Inhalation toxicology*, 19(14): 1135–1146.
- Clay, Karen, Joshua Lewis, and Edson Severnini. 2018. "Pollution, infectious disease, and mortality: evidence from the 1918 Spanish influenza pandemic." *The Journal of Economic History*, 78(4): 1179–1209.
- Cohen, Aaron J, Michael Brauer, Richard Burnett, H Ross Anderson, Joseph Frostad, Kara Estep, Kalpana Balakrishnan, Bert Brunekreef, Lalit Dandona, Rakhi Dandona, et al. 2017. "Estimates and 25-year trends of the global burden of disease attributable to ambient air pollution: an analysis of data from the Global Burden of Diseases Study 2015." *The Lancet*, 389(10082): 1907–1918.
- Cohen, Jon. 2017. "Why flu vaccines so often fail." *Science*: 10.1126/science.aag0105.
- Colmer, Jonathan, Ian Hardman, Jay Shimshack, and John Voorheis. 2020. "Disparities in PM2.5 air pollution in the United States." *Science*, 369(6503): 575–578.
- Correia, Sergio, Paulo Guimarães, and Thomas Zylkin. 2019. "PPMLHDFE: Fast poisson estimation with high-dimensional fixed effects." *arXiv preprint:1903.01690*.
- Cui, Yan, Zuo-Feng Zhang, John Froines, Jinkou Zhao, Hua Wang, Shun-Zhang Yu, and Roger Detels. 2003. "Air pollution and case fatality of SARS in the People's Republic of China: an ecologic study." *Environmental Health*, 2(1): 15.
- Currie, Janet, John Voorheis, and Reed Walker. 2020. "What caused racial disparities in particulate exposure to fall? New evidence from the Clean Air Act and satellite-based measures of air quality." *NBER working paper*.
- de Lataillade, Camille, Stéphane Auvergne, and Isabelle Delannoy. 2009. "2005 and 2006 seasonal influenza vaccination coverage rates in 10 countries in Africa, Asia Pacific, Europe, Latin America and the Middle East." *Journal of public health policy*, 30(1): 83–101.
- Deryugina, Tatyana, Garth Heutel, Nolan H Miller, David Molitor, and Julian Reif. 2019. "The mortality and medical costs of air pollution: Evidence from changes in wind direction." *American Economic Review*, 109(12): 4178–4219.
- Deryugina, Tatyana, Nolan Miller, David Molitor, and Julian Reif. 2021. "Geographic and socioeconomic heterogeneity in the benefits of reducing air pollution in the United States." *Environmental and energy policy and the economy*, 2(1): 157–189.
- Deschenes, Olivier, Michael Greenstone, and Joseph S Shapiro. 2017. "Defensive investments and the demand for air quality: Evidence from the NOx budget program." *American Economic Review*, 107(10): 2958–89.
- Diamond, Gill, Diana Legarda, and Lisa K Ryan. 2000. "The innate immune response of the respiratory epithelium." *Immunological reviews*, 173: 27–38.
- Din, Alexander, and Ron Wilson. 2020. "Crosswalking ZIP Codes to Census Geographies." *Cityscape*, 22(1): 293–314.
- EPA. 2018. *Technical Assistance Document for the Reporting of Daily Air Quality*. United States Environmental Protection Agency.
- EPA. 2020. *Air Quality System Data Mart*. US Environmental Protection Agency.
- Finkelstein, Amy, Sarah Taubman, Bill Wright, Mira Bernstein, Jonathan Gruber, Joseph P Newhouse, Heidi Allen, Katherine Baicker, and Oregon Health Study Group. 2012. "The Oregon health insurance experiment: evidence from the first year." *The Quarterly journal of economics*, 127(3): 1057–1106.
- Flannery, Brendan, Jessie R Chung, Arnold S Monto, Emily T Martin, Edward A Belongia, Huong Q McLean, Manjusha Gaglani, Kempapura Murthy, Richard K Zimmerman, Mary Patricia Nowalk, et al. 2019. "Influenza vaccine effectiveness in the United States during the 2016–2017 season." *Clinical Infectious Diseases*, 68(11): 1798–1806.

- Flannery, Brendan, Rebecca J Garten Kondor, Jessie R Chung, Manjusha Gaglani, Michael Reis, Richard K Zimmerman, Mary Patricia Nowalk, Michael L Jackson, Lisa A Jackson, Arnold S Monto, et al. 2020. "Spread of antigenically drifted influenza A (H3N2) viruses and vaccine effectiveness in the United States during the 2018–2019 season." *The Journal of Infectious Diseases*, 221(1): 8–15.
- Francis, Thomas. 1960. "On the doctrine of original antigenic sin." *Proceedings of the American Philosophical Society*, 104(6): 572–578.
- Gaglani, Manjusha, Jessica Pruszyński, Kempapura Murthy, Lydia Clipper, Anne Robertson, Michael Reis, Jessie R Chung, Pedro A Piedra, Vasanthi Avadhanula, Mary Patricia Nowalk, et al. 2016. "Influenza vaccine effectiveness against 2009 pandemic influenza A (H1N1) virus differed by vaccine type during 2013–2014 in the United States." *The Journal of infectious diseases*, 213(10): 1546–1556.
- GMAO. 2015. *MERRA-2 inst6_3d_ana_Np: 3d,6-Hourly,Instantaneous,Pressure-Level,Analysis,Analyzed Meteorological Fields V5.12.4*. Global Modeling and Assimilation Office (GMAO), Goddard Earth Sciences Data and Information Services Center (GES DISC), Greenbelt, Maryland, USA.
- Gourieroux, Christian, Alain Monfort, Alain Trognon, et al. 1984. "Pseudo Maximum Likelihood Methods: Applications to Poisson Models." *Econometrica*, 52(3): 701–720.
- Greenburg, Leonard, Franklyn Field, Carl L Erhardt, Marvin Glasser, and Joseph I Reed. 1967. "Air pollution, influenza, and mortality in New York city: January-February 1963." *Archives of Environmental Health: An International Journal*, 15(4): 430–438.
- Griffin, Marie R, Arnold S Monto, Edward A Belongia, John J Treanor, Qingxia Chen, Jufu Chen, H Keipp Talbot, Suzanne E Ohmit, Laura A Coleman, Gerry Lofthus, et al. 2011. "Effectiveness of Non-Adjuvanted Pandemic Influenza A Vaccines for Preventing Pandemic Influenza Acute Respiratory Illness Visits in 4 US Communities." *PLoS ONE*, 6(8).
- Hahon, Nicholas, James A Booth, Francis Green, and Trent R Lewis. 1985. "Influenza virus infection in mice after exposure to coal dust and diesel engine emissions." *Environmental research*, 37(1): 44–60.
- Han, Lefei, Jinjun Ran, Yim-Wah Mak, Lorna Kwai-Ping Suen, Paul H Lee, Joseph Sriyal Malik Peiris, and Lin Yang. 2019. "Smoking and influenza-associated morbidity and mortality: a systematic review and meta-analysis." *Epidemiology*, 30(3): 405–417.
- Harper, GJ. 1961. "Airborne micro-organisms: survival tests with four viruses." *Epidemiology & Infection*, 59(4): 479–486.
- HCUP. 2018a. *HCUP State Emergency Department Databases (SEDD)*. Healthcare Cost and Utilization Project, Agency for Healthcare Research and Quality, Rockville, MD.
- HCUP. 2018b. *HCUP State Inpatient Databases (SID)*. Healthcare Cost and Utilization Project, Agency for Healthcare Research and Quality, Rockville, MD.
- Ijaz, M Khalid, Syed A Sattar, C Margaret Johnson-Lussenburg, and VS Springthorpe. 1985. "Comparison of the airborne survival of calf rotavirus and poliovirus type 1 (Sabin) aerosolized as a mixture." *Appl. Environ. Microbiol.*, 49(2): 289–293.
- Iuliano, A Danielle, Katherine M Roguski, Howard H Chang, David J Muscatello, Rakhee Palekar, Stefano Tempia, Cheryl Cohen, Jon Michael Gran, Dena Schanzer, Benjamin J Cowling, et al. 2018. "Estimates of global seasonal influenza-associated respiratory mortality: a modelling study." *The Lancet*, 391(10127): 1285–1300.
- Jackson, Michael L, Jessie R Chung, Lisa A Jackson, C Hallie Phillips, Joyce Benoit, Arnold S Monto, Emily T Martin, Edward A Belongia, Huong Q McLean, Manjusha Gaglani, et al. 2017. "Influenza vaccine effectiveness in the United States during the 2015–2016 season." *New England Journal of Medicine*, 377(6): 534–543.
- Jaspers, Iona, Jonathan M Ciencewicz, Wenli Zhang, Luisa E Brighton, Johnny L Carson, Melinda A Beck, and Michael C Madden. 2005. "Diesel exhaust enhances influenza virus infections in respiratory epithelial cells." *Toxicological Sciences*, 85(2): 990–1002.
- Khare, P, and LC Marr. 2015. "Simulation of vertical concentration gradient of influenza viruses in dust resuspended by walking." *Indoor Air*, 25(4): 428–440.
- Kremer, Michael, and Heidi Williams. 2010. "Incentivizing innovation: Adding to the tool kit." *Innovation policy and the economy*, 10(1): 1–17.

- Lambert, Linda C, and Anthony S Fauci. 2010. "Influenza vaccines for the future." *New England Journal of Medicine*, 363(21): 2036–2044.
- Lee, Greg I, Jordy Saravia, Dahui You, Bishwas Shrestha, Sridhar Jaligama, Valerie Y Hebert, Tammy R Dugas, and Stephania A Cormier. 2014. "Exposure to combustion generated environmentally persistent free radicals enhances severity of influenza virus infection." *Particle and fibre toxicology*, 11(1): 57.
- Liang, Yijia, Liqun Fang, Hui Pan, Kezhong Zhang, Haidong Kan, Jeffrey R Brook, and Qinghua Sun. 2014. "PM 2.5 in Beijing—temporal pattern and its association with influenza." *Environmental Health*, 13(1): 102.
- Lou, Cairong, Hongyu Liu, Yufeng Li, Yan Peng, Juan Wang, and Lingjun Dai. 2017. "Relationships of relative humidity with PM 2.5 and PM 10 in the Yangtze River Delta, China." *Environmental monitoring and assessment*, 189(11): 582.
- Lowen, Anice C, Samira Mubareka, John Steel, and Peter Palese. 2007. "Influenza virus transmission is dependent on relative humidity and temperature." *PLoS Pathog*, 3(10): e151.
- Lu, Peng-Jun, James A Singleton, Gary L Euler, Walter W Williams, and Carolyn B Bridges. 2013. "Seasonal influenza vaccination coverage among adult populations in the United States, 2005–2011." *American journal of epidemiology*, 178(9): 1478–1487.
- McLean, Huong Q, Mark G Thompson, Maria E Sundaram, Burney A Kieke, Manjusha Gaglani, Kempapura Murthy, Pedro A Piedra, Richard K Zimmerman, Mary Patricia Nowalk, Jonathan M Raviotta, et al. 2015. "Influenza vaccine effectiveness in the United States during 2012–2013: variable protection by age and virus type." *The Journal of infectious diseases*, 211(10): 1529–1540.
- Mocko, David, and NASA/GSFC/HSL. 2012. *NLDAS Primary Forcing Data L4 Monthly 0.125 x 0.125 degree V002*. Goddard Earth Sciences Data and Information Services Center (GES DISC), Greenbelt, Maryland, USA.
- Mullins, Jamie T, and Corey White. 2020. "Can access to health care mitigate the effects of temperature on mortality?" *Journal of Public Economics*, 191: 104259.
- NCHS. 2019. *Vital Statistics Data: 1989-2018 Detailed Mortality*. National Center for Health Statistics (NCHS).
- of Labor Statistics, Bureau. 2021. *Local Area Unemployment Statistics (LAUS)*. United States Bureau of Labor Statistics (BLS).
- Ohmit, Suzanne E, Mark G Thompson, Joshua G Petrie, Swathi N Thaker, Michael L Jackson, Edward A Belongia, Richard K Zimmerman, Manjusha Gaglani, Lois Lamerato, Sarah M Spencer, et al. 2014. "Influenza vaccine effectiveness in the 2011–2012 season: protection against each circulating virus and the effect of prior vaccination on estimates." *Clinical infectious diseases*, 58(3): 319–327.
- Putri, Wayan CWS, David J Muscatello, Melissa S Stockwell, and Anthony T Newall. 2018. "Economic burden of seasonal influenza in the United States." *Vaccine*, 36(27): 3960–3966.
- Quinn, Sandra Crouse, Supriya Kumar, Vicki S Freimuth, Donald Musa, Nestor Casteneda-Angarita, and Kelley Kidwell. 2011. "Racial disparities in exposure, susceptibility, and access to health care in the US H1N1 influenza pandemic." *American journal of public health*, 101(2): 285–293.
- Rivas-Santiago, César E, Srijata Sarkar, Pasquale Cantarella, Álvaro Osornio-Vargas, Raúl Quintana-Belmares, Qingyu Meng, Thomas J Kirn, Pamela Ohman Strickland, Judith C Chow, John G Watson, et al. 2015. "Air pollution particulate matter alters antimycobacterial respiratory epithelium innate immunity." *Infection and immunity*, 83(6): 2507–2517.
- Rolfes, Melissa A, Brendan Flannery, Jessie R Chung, Alissa O'Halloran, Shikha Garg, Edward A Belongia, Manjusha Gaglani, Richard K Zimmerman, Michael L Jackson, Arnold S Monto, et al. 2019. "Effects of influenza vaccination in the United States during the 2017–2018 influenza season." *Clinical Infectious Diseases*, 69(11): 1845–1853.
- Schiller, Jeannine S, and GL Euler. 2009. "Vaccination coverage estimates from the National Health Interview Survey: United States, 2008." *National Center for Health Statistics (NCHS). Health E-Stat. Centers for Disease Control and Prevention (CDC)*.
- Shaman, Jeffrey, and Melvin Kohn. 2009. "Absolute humidity modulates influenza survival, transmission, and seasonality." *Proceedings of the National Academy of Sciences*, 106(9): 3243–3248.

- Shaman, Jeffrey, Virginia E Pitzer, Cécile Viboud, Bryan T Grenfell, and Marc Lipsitch.** 2010. "Absolute humidity and the seasonal onset of influenza in the continental United States." *PLoS Biol*, 8(2): e1000316.
- Silva, JMC Santos, and Silvana Tenreiro.** 2006. "The log of gravity." *The Review of Economics and statistics*, 88(4): 641–658.
- Silva, JMC Santos, and Silvana Tenreiro.** 2011. "Further simulation evidence on the performance of the Poisson pseudo-maximum likelihood estimator." *Economics Letters*, 112(2): 220–222.
- Stoecker, Charles, Nicholas J Sanders, and Alan Barreca.** 2016. "Success Is something to sneeze at: Influenza mortality in cities that participate in the Super Bowl." *American Journal of Health Economics*, 2(1): 125–143.
- Tellier, Raymond.** 2009. "Aerosol transmission of influenza A virus: a review of new studies." *Journal of the Royal Society Interface*, 6(suppl.6): S783–S790.
- Treanor, John J, H Keipp Talbot, Suzanne E Ohmit, Laura A Coleman, Mark G Thompson, Po-Yung Cheng, Joshua G Petrie, Geraldine Lofthus, Jennifer K Meece, John V Williams, et al.** 2012. "Effectiveness of seasonal influenza vaccines in the United States during a season with circulation of all three vaccine strains." *Clinical infectious diseases*, 55(7): 951–959.
- Tschofen, Peter, Inês L Azevedo, and Nicholas Z Muller.** 2019. "Fine particulate matter damages and value added in the US economy." *Proceedings of the National Academy of Sciences*, 116(40): 19857–19862.
- United States Census Bureau.** 2018. *2018 FIPS Codes*. United States Census Bureau.
- Ward, Courtney J.** 2014. "Influenza vaccination campaigns: is an ounce of prevention worth a pound of cure?" *American Economic Journal: Applied Economics*, 6(1): 38–72.
- White, Corey.** 2019. "Measuring Social and Externality Benefits of Influenza Vaccination." *Journal of Human Resources*.
- Wolkoff, Peder.** 2018. "Indoor air humidity, air quality, and health—An overview." *International journal of hygiene and environmental health*, 221(3): 376–390.
- Wong, Chit Ming, Lin Yang, Thuan Quoc Thach, Patsy Yuen Kwan Chau, King Pan Chan, G Neil Thomas, Tai Hing Lam, Tze Wai Wong, Anthony J Hedley, and JS Malik Peiris.** 2009. "Modification by influenza on health effects of air pollution in Hong Kong." *Environmental health perspectives*, 117(2): 248–253.
- Wu, Xiao, Rachel C. Nethery, Benjamin M. Sabath, Danielle Braun, and Francesca Dominici.** 2020. "Exposure to air pollution and COVID-19 mortality in the United States." *medRxiv preprint: 10.1101/2020.04.05.20054502*, , (10.1101/2020.04.05.20054502).
- Xia, Youlong, Kenneth Mitchell, Michael Ek, Justin Sheffield, Brian Cosgrove, Eric Wood, Lifeng Luo, Charles Alonge, Helin Wei, Jesse Meng, et al.** 2012. "Continental-scale water and energy flux analysis and validation for the North American Land Data Assimilation System project phase 2 (NLDAS-2): 1. Intercomparison and application of model products." *Journal of Geophysical Research: Atmospheres*, 117(D3).
- Zhang, Jun, and F Yu Kai.** 1998. "What's the relative risk?: A method of correcting the odds ratio in cohort studies of common outcomes." *Jama*, 280(19): 1690–1691.
- Zimmerman, Richard K, Mary Patricia Nowalk, Jessie Chung, Michael L Jackson, Lisa A Jackson, Joshua G Petrie, Arnold S Monto, Huong Q McLean, Edward A Belongia, Manjusha Gaglani, et al.** 2016. "2014–2015 Influenza Vaccine Effectiveness in the United States by Vaccine Type." *Clinical Infectious Diseases: An Official Publication of the Infectious Diseases Society of America*, 63(12): 1564.

APPENDIX FOR ONLINE PUBLICATION

When Externalities Collide: Influenza and Pollution

by Joshua Graff Zivin^{1,2,*}, Matthew Neidell^{3,2,*}, Nicholas J. Sanders^{4,2,*}, Gregor Singer^{5,*}

¹University of California, San Diego

²National Bureau of Economic Research

³Columbia University

⁴Cornell University

⁵London School of Economics

*Correspondence to: Joshua Graff Zivin: jgraffzivin@ucsd.edu, Matthew Neidell: mn2191@cumc.columbia.edu,
Nicholas J. Sanders: njsanders@cornell.edu, Gregor Singer: g.a.singer@lse.ac.uk

A.1 Additional Descriptive Statistics

Table A.1 contains states and years with available admission months and patient zip codes in the [HCUP \(2018b\)](#) inpatient hospitalization data we use. Figure A.1 plots distributions of several socio-demographic variables for the counties in our HCUP data and for all U.S. counties. The graphs show similar distributions suggesting that the subset of HCUP counties is broadly representative of U.S. counties. Table A.2 contains summary statistics at the county-year-month level for inpatient hospital admissions with a primary influenza diagnosis, associated hospital charges, and the average monthly AQI. We use the standard deviation of the AQI during the influenza season (10.9), the average inpatient hospitalization admissions (4.04) and charges (117,000 US\$) for the calculation of absolute effects based on our Poisson GMM-IV estimates.

To further illustrate the influenza seasonality, we use data on the timing of national influenza-like illnesses from the Centers for Disease Control and Prevention ([CDC 2020](#)). Figure A.2 shows that the seasonality of inpatient hospitalizations in our data matches closely with general influenza-like illnesses reported by the CDC.

The AQI is based on multiple pollutants, but for each county-day, a single pollutant is the defining pollutant of the AQI ([EPA 2018](#)). Figure A.3 shows which pollutants are the main defining pollutants of the AQI during the influenza season from October through March for three different intervals covering our sample. Particulate matter (PM_{2.5} and PM₁₀) and ozone are the defining pollutants in the AQI for the majority of cases in each time period.

Table A.1: Data coverage with available zip codes and admission months

Arizona	2007,2008,2009,2010,2011,2012,2013,2014,2015,2016,2017
Arkansas	2009
Colorado	2007,2008,2009,2010,2011,2012
Hawaii	2009
Iowa	2009
Kentucky	2007,2008,2009,2010,2011,2012,2013,2014
Maryland	2009,2010,2011,2012
Massachusetts	2007,2008,2009,2010,2011,2012,2013,2014
Michigan	2008,2009,2010,2011,2012,2013,2014,2015,2016,2017
Minnesota	2014,2015,2016
Nevada	2010,2011,2012,2013,2014,2015
New Jersey	2007,2008,2009,2010,2011,2012,2013,2014,2015,2016,2017
New York	2007,2008,2009,2010,2011,2012,2013,2014,2015
North Carolina	2008,2009,2010,2011,2012,2013,2014,2015,2016,2017
Oregon	2008,2009
Rhode Island	2007,2008,2009,2010,2011,2012,2013,2014,2015
South Dakota	2009
Utah	2009
Vermont	2009
Washington	2007,2008,2009,2010,2011,2012,2013,2014,2015,2016,2017
Wisconsin	2009

Notes: The table shows the states and years with available admission month and patient zip code used in the analysis for influenza hospitalizations.

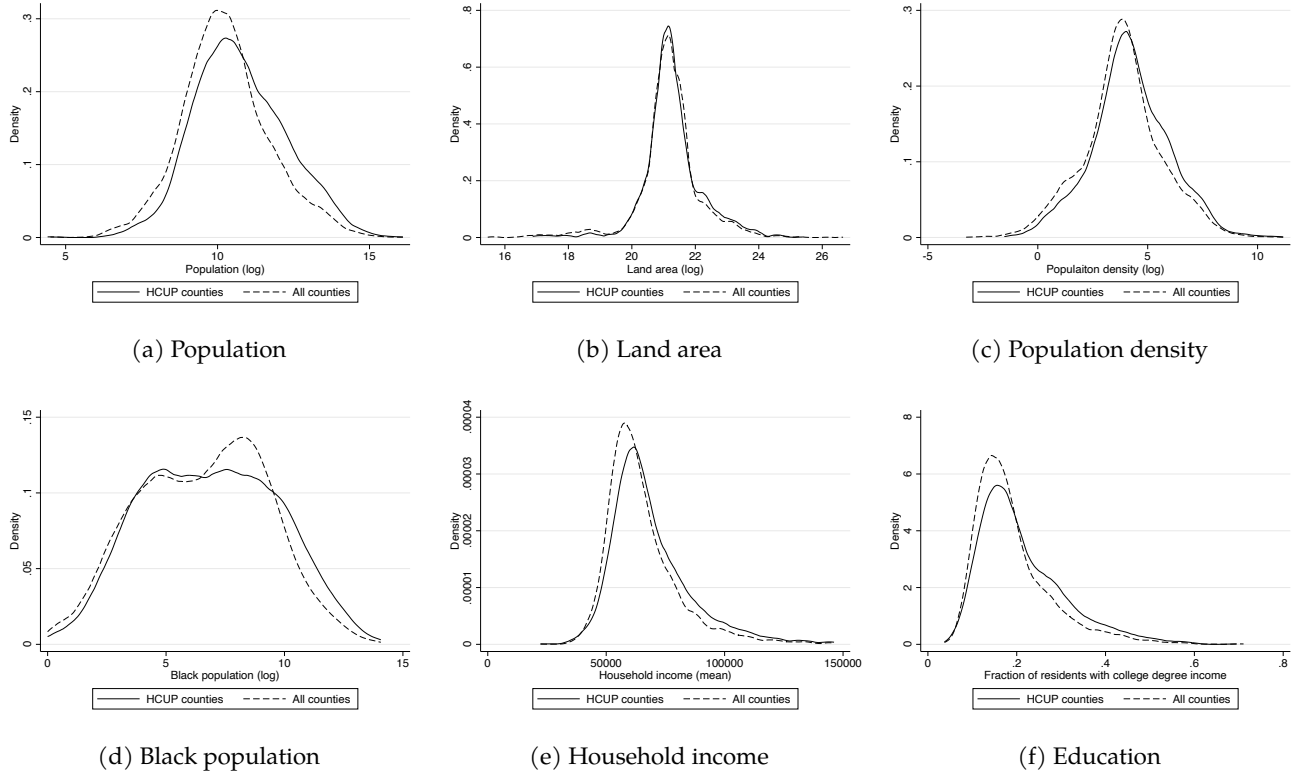


Figure A.1: Comparing distributions of HCUP counties and all U.S. counties

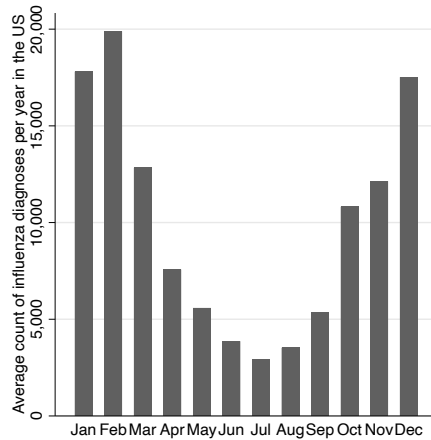
Notes: The graphs show the kernel densities of the indicated variables across counties, separately for counties that are part of our HCUP sample, and all U.S. counties. All variables are taken from the 2010 U.S. Census and from [Chetty et al. \(2018\)](#) and correspond to year 2010, except household income which corresponds to year 2000.

Table A.2: Summary statistics of influenza hospitalizations and air pollution (AQI)

		Mean	SD	Min	5th p.	10th p.	25th p.	75th p.	90th p.	95th p.	Max
Hospital admissions per county per month	Oct-Mar	4.04	16.3	0	0	0	0	2	8	17	588
	Apr-Sep	0.526	3.41	0	0	0	0	0	1	2	170
Hospital charges (th. USD) per county per month	Oct-Mar	117	567	0	0	0	0	39.1	202	503	23729
	Apr-Sep	16.7	124	0	0	0	0	0	18	57.5	6883
Average AQI across county-months	Oct-Mar	34.5	10.9	7.14	16.3	21	28	40.6	47.3	52.9	72.4
	Apr-Sep	42.9	14.1	11.3	17.8	23.5	35.2	50.2	59.7	67.6	84.8

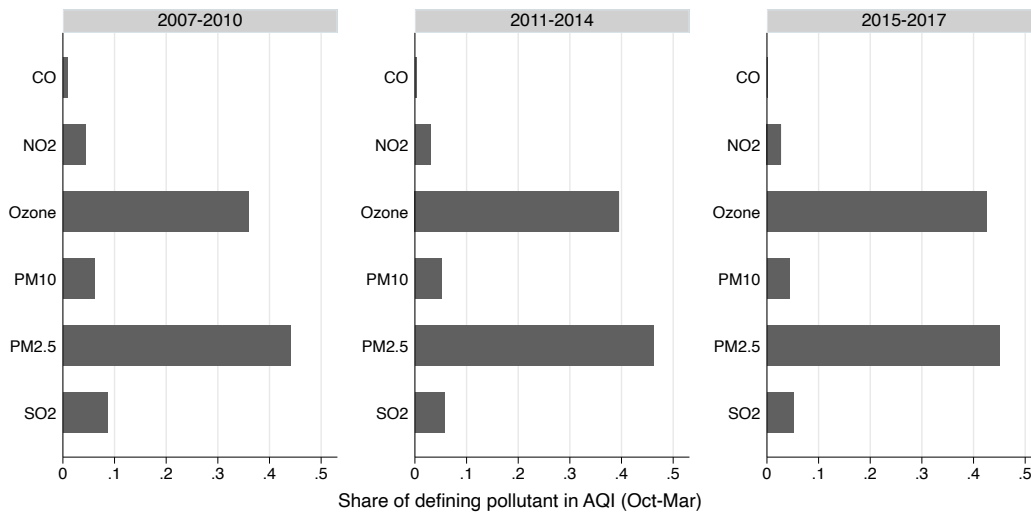
Notes: The table shows summary statistics for influenza diagnosed inpatient hospital admissions and charges, and air pollution measured by the AQI. We pool and report data separately by the influenza season of October through March and the off season of April through September. The AQI statistics are based on the coverage of the hospitalization sample. The reported means in the regression tables may diverge due to dropping of observations without variation in the outcome variable for estimation.

Figure A.2: Influenza-like illnesses in U.S.



Notes: The figure shows the distribution of recorded influenza-like illnesses from [CDC \(2020\)](#), which includes non-hospitalized cases. Data are pooled across the U.S. spanning 1997-2019. Not all health providers report to the Influenza-Like Illness (ILI) Network, and the number of providers reporting grew over time so total number of cases is a lower bound of true infection rates.

Figure A.3: Defining pollutants of the AQI



Notes: The figure shows each pollutant's share in days when it was the defining pollutant for calculating the AQI at the county-day level. The shares in days are calculated for the three to four year periods as indicated and are based on the months of the influenza season (Oct-Mar). The data on defining pollutants comes from [EPA \(2020\)](#).

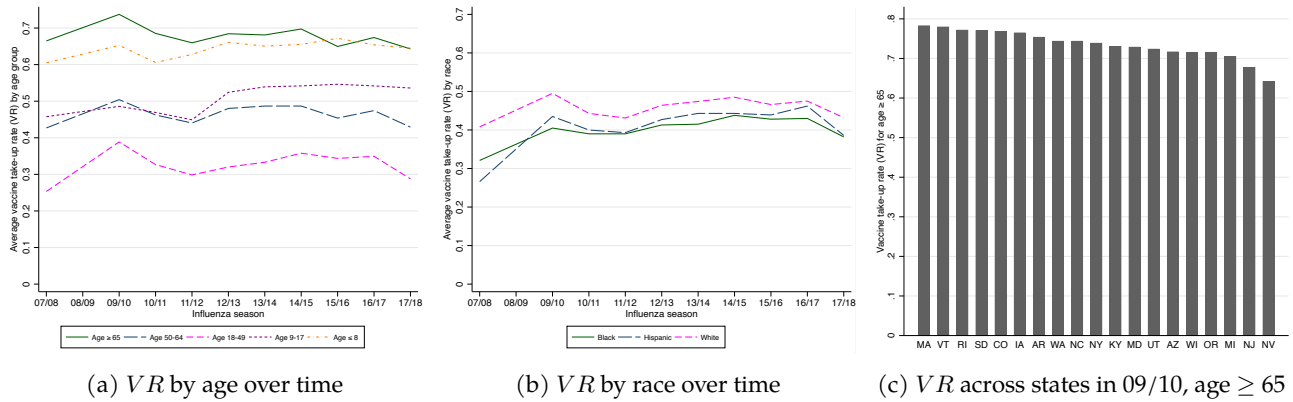


Figure A.4: Vaccine take-up rates over time and across states

Notes: Panel (a) shows vaccine take-up rates by age group averaged across states, and Panel (b) by race averaged across states. Panel (c) shows vaccine take-up rates for age group 65 years and older in 2009/2010 for different states.

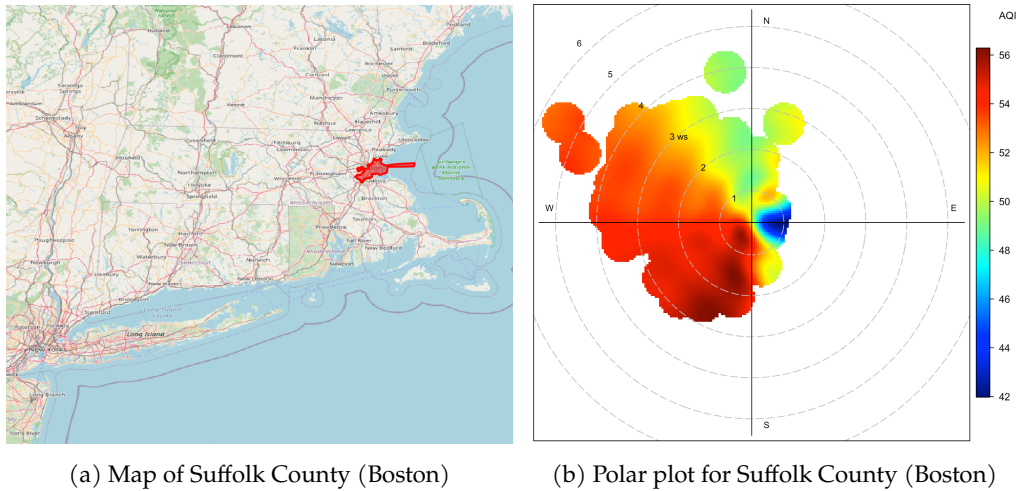


Figure A.5: Prevailing wind direction and air pollution: Suffolk County (Boston)

Notes: Panel (a) shows a map of Suffolk County (Boston) and surrounding areas, e.g. New York City to the South-West. Panel (b) shows a calculated polar plot of monthly air pollution (AQI) levels, where a deeper red means higher pollution. The polar plot shows the average pollution (color) when monthly prevailing winds blow from a particular direction (clockwise) and with a particular wind speed (outwards for higher speeds).

A.2 Econometric details

In this section we detail how we estimate our Poisson GMM-IV model with fixed effects. To simplify notation, we index observations by i and collect all variables on the right hand side of Equation (2) into \mathbf{X}_i except the fixed effects γ_i^j at the county-by-year-by-month level j with total observations $J = \sum_{i \in j}$ per fixed effect cell. The conditional mean of hospitalization counts H_i is given by:

$$E[H_i | \mathbf{X}_i, \gamma_i^j] = g(\mathbf{X}_i \beta + \gamma_i^j) = \alpha_i^j \exp(\mathbf{X}_i \beta) \quad (7)$$

where \mathbf{X}_i are the AQI, control variables, as well as year by month dummies. In our baseline exponential mean specification consistent with a Poisson count model, the function $g(\cdot)$ is the exponential function $\exp(\cdot)$, such that we can rewrite $g(\mathbf{X}_i \beta + \gamma_i^j) = \alpha_i^j \exp(\mathbf{X}_i \beta)$, where $\alpha_i^j = g(\gamma_i^j)$. In our linear mean specification, the function $g(\cdot)$ is just a linear function, i.e. the argument itself. We use a general methods of moments (GMM) estimator using standard moment conditions:

$$E[\epsilon_i | \mathbf{Z}_i] = 0 \quad (8)$$

where \mathbf{Z}_i are instruments and ϵ_i the errors. Note that we do not require any additional distributional assumptions for consistency of β , only that the conditional mean function is correctly specified and that our moment conditions hold. When our instruments \mathbf{Z}_i are the variables themselves (\mathbf{X}_i), our GMM estimator is numerically equivalent to a standard fixed effects Poisson Pseudo-Maximum Likelihood (PPML) estimator.

We account for fixed effects γ_i^j by first defining $\bar{H}_i^j = J^{-1} \sum_{i \in j} H_i$ as the average count of hospitalizations within a county-season-year cell j corresponding to the level of our county-year-season fixed effect γ_i^j , i.e. averaging across months in each cell. Next, note that γ_i^j or α_i^j does not vary across observations i at the fixed effect level j , and therefore:

$$E[\bar{H}_i^j | \mathbf{X}_i, \gamma_i^j] = J^{-1} \sum_{i \in j} g(\mathbf{X}_i \beta + \gamma_i^j) = J^{-1} \sum_{i \in j} \alpha_i^j g(\mathbf{X}_i \beta) = \alpha_i^j J^{-1} \sum_{i \in j} g(\mathbf{X}_i \beta) = \alpha_i^j \bar{g}_i^j(\beta) \quad (9)$$

The last equality defines $\bar{g}_i^j(\beta) = J^{-1} \sum_{i \in j} g(\mathbf{X}_i \beta)$. The key insight is that:

$$\alpha_i^j \equiv g(\gamma_i^j) = E \left[\frac{\bar{H}_i^j}{\bar{g}_i^j(\beta)} | \mathbf{X}_i, \gamma_i^j \right] \quad (10)$$

Combining Equations (7), (8) and (10) yields an expression for the moment conditions that re-

moves the fixed effect through quasi-mean differencing:

$$E[\epsilon_i | \mathbf{Z}_i] = E[H_i - \alpha_i^j \bar{g}_i^j(\mathbf{X}_i) | \mathbf{Z}_i] = E \left[H_i - \frac{\bar{H}_i^j}{\bar{g}_i^j(\beta)} g(\mathbf{X}_i \beta) | \mathbf{Z}_i \right] = 0 \quad (11)$$

Since $\bar{g}_i^j(\beta)$ is a function of β , it needs to be recomputed in every iteration of the GMM algorithm. Defining residuals as $\hat{\epsilon}_i$, the empirical moment conditions are:

$$E[\mathbf{Z}_i' \hat{\epsilon}_i] = 0 \quad (12)$$

Dropping subscripts, β minimizes the GMM objective function Q :

$$\beta = \arg \min_{\beta} Q = (\mathbf{Z}' \hat{\epsilon})' \mathbf{W} (\mathbf{Z}' \hat{\epsilon}) \quad (13)$$

where $\mathbf{W} = (\frac{1}{N} \mathbf{Z}' \mathbf{Z})^{-1}$ is a weighting matrix. We compute clustered standard errors using the covariance matrix of β :

$$VCOV(\beta) = \frac{1}{N} (\mathbf{G}' \mathbf{W} \mathbf{G})^{-1} \mathbf{G}' \mathbf{W} \mathbf{S} \mathbf{W} \mathbf{G} (\mathbf{G}' \mathbf{W} \mathbf{G})^{-1} \quad (14)$$

where $\mathbf{S} = \frac{1}{N} \sum_j \sum_{i \in j} (\mathbf{Z}_i' \hat{\epsilon}_i) (\mathbf{Z}_i' \hat{\epsilon}_i)'$ and $\mathbf{G} = \frac{1}{N} \sum_i \mathbf{Z}_i' \frac{\partial \epsilon_i}{\partial \beta'}$. In our empirical application, we use a fixed effect demeaned version of our instrument matrix \mathbf{Z}_i to match the instruments that would be used in a two stage least squares regression, which we denote $\tilde{\mathbf{Z}}_i = \mathbf{Z}_i - J^{-1} \sum_{i \in j} \mathbf{Z}_i$.⁵⁰ We use a two-step optimal GMM procedure where we use S^{-1} from the first step as weighting matrix for the second step.

Finally, for robustness checks, we use a linear conditional mean function instead of an exponential conditional mean function where H_i is either the count of hospitalizations or the inverse hyperbolic sine (IHS) of hospitalizations counts:

$$E[H_i | \mathbf{X}_i, \gamma_i^j] = \mathbf{X}_i \beta + \gamma_i^j \quad (15)$$

This changes the moment conditions in Equation (11) to a standard mean-differenced version for linear GMM:

$$E[\epsilon_i | \mathbf{Z}_i] = E \left[(H_i - \bar{H}_i^j) - (\mathbf{X}_i - \bar{\mathbf{X}}_i^j) \beta | \mathbf{Z}_i \right] = 0 \quad (16)$$

⁵⁰In practices, it makes little difference whether we use $\tilde{\mathbf{Z}}_i$ or \mathbf{Z}_i .

A.3 Additional tables

Table A.3: First stage results

	Wind IVs			Inversion IVs			Wind + Inversion IVs		
	AQI (1)	AQI (2)	AQI X EVT (3)	AQI (4)	AQI (5)	AQI X EVT (6)	AQI (7)	AQI (8)	AQI X EVT (9)
Z^{NE}	.47 (.042)	.47 (.089)	.011 (.022)				.47 (.042)	.45 (.089)	.006 (.022)
Z^{SE}	.72 (.035)	.83 (.09)	.055 (.015)				.72 (.035)	.79 (.09)	.047 (.015)
Z^{SW}	.5 (.058)	.71 (.11)	.013 (.022)				.48 (.058)	.68 (.11)	.013 (.022)
Z^{NW}	.56 (.066)	1.1 (.17)	.11 (.026)				.56 (.066)	1.1 (.17)	.11 (.026)
$Z^{NE} \times VE$.0045 (.41)	.25 (.11)					.025 (.41)	.25 (.11)
$Z^{SE} \times VE$		-.35 (.26)	.25 (.056)					-.26 (.26)	.28 (.055)
$Z^{SW} \times VE$		-.74 (.41)	.25 (.095)					-.69 (.42)	.25 (.096)
$Z^{NW} \times VE$		-1.7 (.44)	-.071 (.086)					-1.7 (.45)	-.075 (.087)
InvDays X \overline{AQI}				.54 (.13)	1 (.3)	.06 (.063)	.47 (.12)	.88 (.26)	.045 (.061)
InvDays				-15 (4.6)	-37 (11)	-3.1 (2.2)	-12 (4.2)	-31 (9.2)	-2.5 (2.1)
InvStr X \overline{AQI}				.021 (.02)	.081 (.062)	.0087 (.0095)	.018 (.018)	.054 (.05)	.0049 (.0086)
InvStr				-.55 (.71)	-3 (2.2)	-.39 (.34)	-.52 (.65)	-2.2 (1.8)	-.28 (.3)
InvDays X \overline{AQI} X VE					-1.4 (1)	.095 (.26)		-1.2 (.94)	.11 (.25)
InvDays X VE					66 (35)	1.9 (8.7)		54 (32)	1.1 (8.5)
InvStr X \overline{AQI} X VE					-.16 (.16)	-.013 (.03)		-.097 (.14)	-.0038 (.029)
InvStr X VE					6.6 (5.7)	.85 (1.1)		4.6 (4.8)	.54 (1)
Observations	17668	17668	17668	17668	17668	17668	17668	17668	17668
F (K-P)	176.8	35.3	35.3	8.6	3.1	3.1	91	20.9	20.9
F (S-W)	176.8	93.2	73.9	8.6	8.7	8.0	91	48.1	38.6

Notes: The table shows first stage results by using linear regressions of the endogenous variables on our instruments, controls and fixed effects. Columns (1), (4) and (7) show the results from our model with one endogenous variables (without interacting with VP) in Equation (2). The other Columns show first stage results from our model with two endogenous variables (with interacting with VP) in Equation (5). The dependent variables are the endogenous variables indicated at the top of the table. In Columns (1) to (3) we use our instruments based on wind directions. In Columns (4) to (6) we use our instruments based on thermal inversions. In Columns (7) to (9) we use our both our instruments based on wind directions and thermal inversions. We limit analysis to the influenza intensive months of October through March and our sample spans 2007-2017 with the exception of October 2008 to March 2009 where vaccine effectiveness data is not available. Vaccine effectiveness is weighted by average vaccination rates and hospitalization shares across age groups and is measured between 0 (low) and 1 (high). The results are from a Ordinary Least Squares regression with county-by-season-by-year and year-by-month fixed effects as well as weather controls. Weather controls consist of five bins of temperature quintiles, five bins of specific humidity quintiles, and linear terms for precipitation and wind speed. All weather variables are based on county-year-month averages. Standard errors in parentheses are clustered at the county level.

Table A.4: Monte Carlo simulation on convergence of first stage coefficients to one

Number of years	Bias of first stage coefficients						
	Number of counties						
	25	50	100	200	500	1000	3000
4	86%	88%	53%	33%	12%	11%	5%
5	59%	36%	22%	15%	8%	4%	3%
6	42%	26%	17%	11%	9%	5%	3%
7	37%	17%	17%	7%	7%	5%	2%
8	28%	21%	12%	7%	5%	3%	2%
10	21%	15%	9%	6%	4%	3%	2%
15	16%	11%	6%	5%	3%	2%	1%
20	11%	9%	4%	3%	2%	2%	1%

Notes: The table shows a Monte Carlo simulation of the maximum bias in the first stage coefficients in the model with one endogenous variables (without interacting with VP) in Equation (2). The bias estimates are created by simulating a dataset with the number of years and counties as indicated with 6 months per year. We populate the data randomly with AQI values, based on a normal distribution with mean and variance of our original data, and winsorizing the maximum and minimum to the maximum and minimum from our original AQI data. We randomly populate the data with wind direction bins from a uniform distribution from 1.1 to 4.1, which we then round to the nearest integer, such that there are four bins and some wind direction bins $WindDirBin$ occur more frequently (but randomly across the entire sample). To generate some correlation between AQI and wind direction bins, we multiply the AQI with $\log(WindDirBin + 1.5) \times (\log(CountyIndicator + 2)/3)$ for the first half of the counties and with $1/\log(WindDirBin + 1.5) \times (\log(CountyIndicator + 2)/3)$ for the second half of counties. We then calculate the instrument as described in our paper, and run first stage regressions based on Equation (2) omitting all control variables, except our fixed effects. We note the maximum percentage deviation from any of the coefficients of the instruments in the first stage as $(1/\beta - 1) \times 100\%$. We repeat the simulation 20 times for each county-year configuration and show the average of the maximum percentage deviation in the above table. The table shows that as either the number of counties, or the number of years increases, the first stage coefficients converge to one. The exact size of the deviations are not directly comparable to our estimates, as we are, for example, including control variables, but the convergence patterns should apply.

Table A.5: Reduced form using vaccine effectiveness (VE) directly

	Poisson GMM		Poisson GMM-IV	
	(1)	(2)	(3)	(4)
AQI	.0076 (.0024)	.035 (.0078)	.028 (.0074)	.099 (.021)
AQI X VE		-.082 (.022)		-.28 (.079)
Observations	17668	17668	17668	17668
Mean of outcome	6.04	6.04	6.04	6.04
Mean of AQI	35.27	35.27	35.27	35.27
Mean of VE	-	0.36	-	0.36

Notes: The dependent variable is the count of inpatient hospital admissions with influenza as primary diagnosis within a county-year-month. We limit analysis to the influenza intensive months of October through March and our sample spans 2007-2017 with the exception of October 2008 to March 2009 where vaccine effectiveness data is not available. Instead of using vaccine protection (VP), we use vaccine effectiveness (VE) directly. Vaccine effectiveness is weighted by average vaccination rates and hospitalization shares across age groups and is measured between 0 (low) and 1 (high). The results are from a Poisson-GMM estimation with county-by-season-by-year fixed effects and year-by-month dummies as well as weather controls. Weather controls consist of five bins of temperature quintiles, five bins of specific humidity quintiles, and linear terms for precipitation and wind speed. All weather variables are based on county-year-month averages. The air quality index (AQI) is lagged one month and a higher AQI means worse air quality. The columns indicating "GMM-IV" use our instruments based on wind direction instead of the AQI to generate moment conditions, and in even-numbered columns use the interaction between wind direction instruments and vaccine effectiveness (VE). Standard errors in parentheses are clustered at the county level.

Table A.6: Heterogeneity by age and race (without instruments)

	≤ 8y		9-64y		≥ 65y		Black/Hispanic		White	
	(1)	(2)	(3)	(4)	(5)	(6)	(7)	(8)	(9)	(10)
AQI	.0075 (.0027)	.015 (.011)	.0096 (.0032)	.011 (.0075)	.0035 (.0025)	.025 (.0056)	.0087 (.0041)	.045 (.013)	.0092 (.0021)	.034 (.007)
AQI X VP		-.025 (.035)		-.0088 (.038)		-.11 (.028)		-.18 (.058)		-.11 (.032)
Observations	10593	10593	13984	13984	13619	13619	7740	7740	15553	15553
Mean of outcome	1.89	1.89	2.76	2.76	3.51	3.51	3.27	3.27	4.17	4.17
Mean of AQI	36.51	36.51	35.7	35.7	35.5	35.5	37.5	37.5	35.46	35.46
Mean of VP	-	0.31	-	0.16	-	0.2	-	0.21	-	0.23
Mean of VE	-	0.48	-	0.4	-	0.3	-	0.36	-	0.37

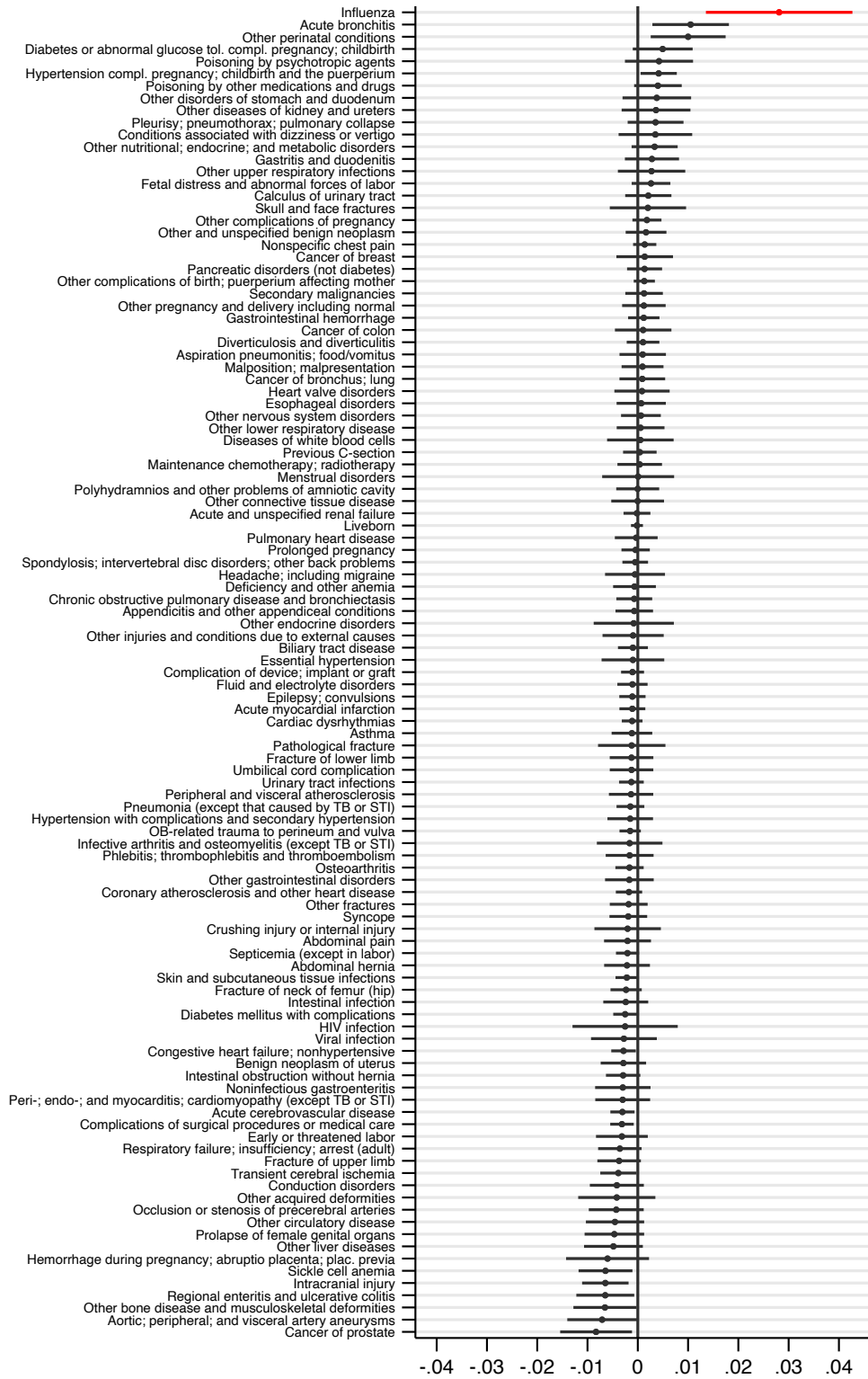
Notes: The dependent variable is the count of inpatient hospital admissions with influenza as primary diagnosis within a county-year-month. The columns indicate which age or race subgroups are counted in the dependent variable. We limit analysis to the influenza intensive months of October through March and our sample spans 2007-2017 with the exception of October 2008 to March 2009 where vaccine effectiveness data is not available. Vaccine protection (VP) is weighted by hospitalization shares across age groups and is measured between 0 (low) and 1 (high). We only use the vaccine take-up rates and raw vaccine effectiveness for the age groups indicated in each column. For the results by racial groups, we use our VP scaled by the ratio of race specific to overall vaccine take-up by season. The results are from Poisson GMM estimations without instruments with county-by-season-by-year fixed effects and year-by-month dummies as well as weather controls. Weather controls consist of five bins of temperature quintiles, five bins of specific humidity quintiles, and linear terms for precipitation and wind speed. All weather variables are based on county-year-month averages. The air quality index (AQI) is lagged one month and a higher AQI means worse air quality. The number of included observations can vary across different outcomes due to fixed effects and varied counts in each county-year-month cell. Standard errors in parentheses are clustered at the county level.

Table A.7: Further robustness: PPML, and linear model with IHS of counts

	Poisson GMM		PPML		OLS/Lin. GMM (IHS)		Lin. GMM-IV (IHS)	
	(1)	(2)	(3)	(4)	(5)	(6)	(7)	(8)
AQI	.0076 (.0024)	.034 (.0076)	.0076 (.0024)	.034 (.0076)	.0043 (.0012)	.0094 (.0039)	.02 (.0051)	.038 (.012)
AQI X VP		-.14 (.036)		-.14 (.036)		-.024 (.017)		-.11 (.066)
Observations	17668	17668	17668	17668	17668	17668	17668	17668
Mean of outcome	6.04	6.04	6.04	6.04	1.34	1.34	1.34	1.34
Mean of AQI	35.27	35.27	35.27	35.27	35.27	35.27	35.27	35.27
Mean of VP	-	0.21	-	-	-	0.21	-	0.21
Mean of VE	-	0.36	-	-	-	0.36	-	0.36

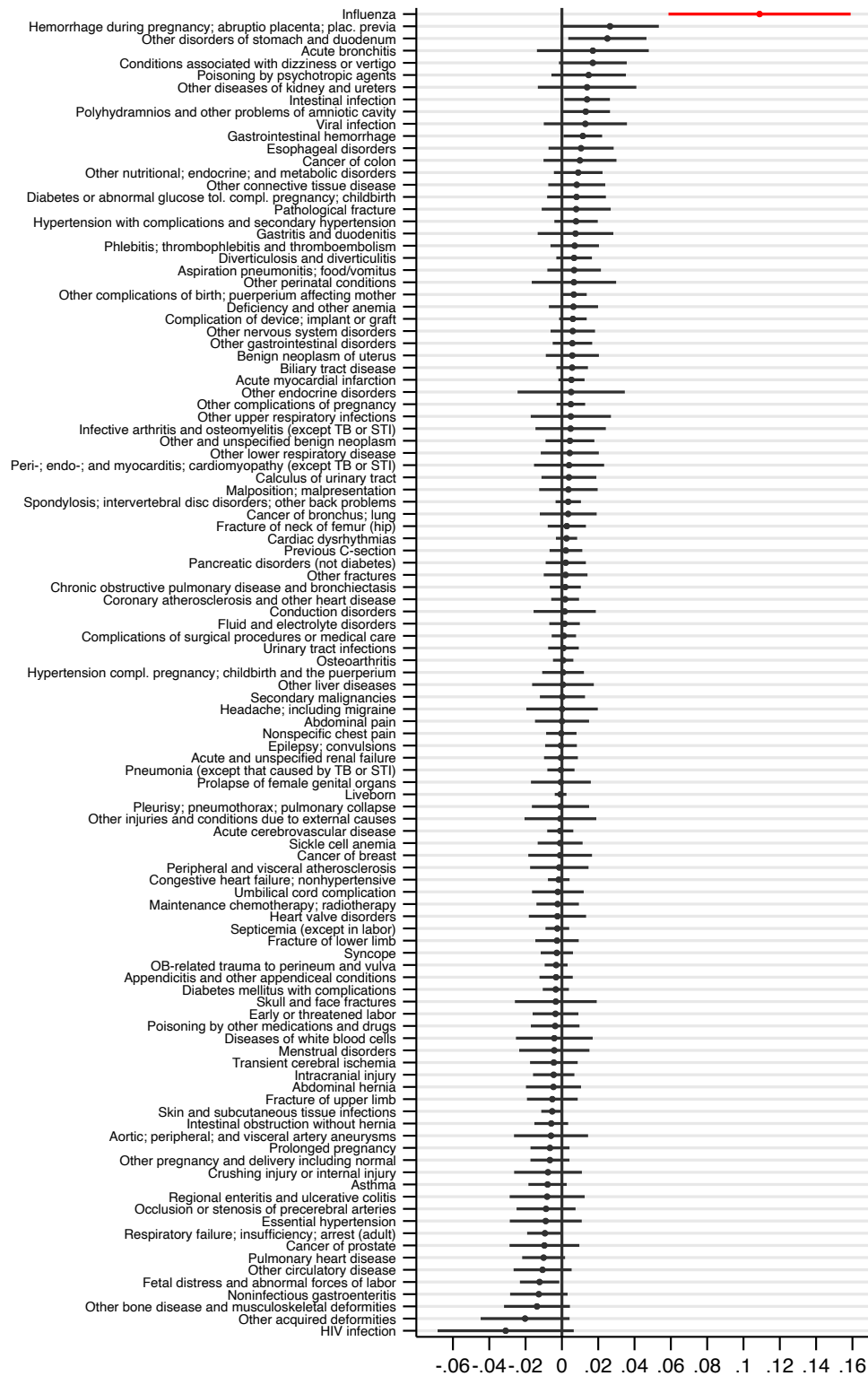
Notes: The dependent variable is the count of inpatient hospitalizations with influenza as primary diagnosis in Columns (1) to (4), and the inverse hyperbolic sine (IHS) of the count of inpatient hospitalizations with influenza as primary diagnosis in Columns (5) to (8), all at the county-year-month level. We limit analysis to the influenza intensive months of October through March and our sample spans 2007-2017 with the exception of October 2008 to March 2009 where vaccine effectiveness data is not available. Vaccine protection (VP) is weighted by hospitalization shares across age groups and is measured between 0 (low) and 1 (high). The results are from a Poisson GMM estimation in Columns (1) and (2), from a Poisson Pseudo-Maximum Likelihood (PPML) in Columns (3) and (4), and from a linear GMM estimation in Columns (5) to (8), all with county-by-season-by-year fixed effects and year-by-month dummies as well as weather controls. Weather controls consist of five bins of temperature quintiles, five bins of specific humidity quintiles, and linear terms for precipitation and wind speed. All weather variables are based on county-year-month averages. The air quality index (AQI) is lagged one month and a higher AQI means worse air quality. Columns (7) and (8) indicating “GMM-IV” use our instruments based on wind direction instead of the AQI to generate moment conditions, and in Column (8) we additionally use our VE instrument instead of VP to form moment conditions. Standard errors in parentheses are clustered at the county level.

Figure A.6: Effect of AQI on various diseases (baseline AQI)



Notes: The figure shows the estimates and confidence intervals of AQI using Equation (2) and several outcomes that have a primary diagnosis as indicated. We use the Clinical Classifications Software (CCS) from the Agency for Healthcare Research and Quality (AHRQ) to classify the relevant ICD code groupings (around 250 groups), and plot the results for all CCS groupings where the mean of the outcome is at least 3.02, half the mean of our influenza outcome (6.04), to ensure there are enough cases in our outcome. The p-values are not adjusted for the family wise error rate. The associated q-values from a Holm-Bonferroni correction are all above 0.1 except for influenza as outcome.

Figure A.7: Effect of AQI on various diseases (in interaction model)



Notes: The figure shows the estimates and confidence intervals of AQI using Equation (5) and several outcomes that have a primary diagnosis as indicated. We use the Clinical Classifications Software (CCS) from the Agency for Healthcare Research and Quality (AHRQ) to classify the relevant ICD code groupings (around 250 groups), and plot the results for all CCS groupings where the mean of the outcome is at least 3.02, half the mean of our influenza outcome (6.04), to ensure there are enough cases in our outcome. The p-values are not adjusted for the family wise error rate. The associated q-values from a Holm-Bonferroni correction are all above 0.1 except for influenza as outcome.

Figure A.8: Effect of AQIxVE on various diseases (in interaction model)



Notes: The figure shows the estimates and confidence intervals of the interaction term of AQI and VE using Equation (5) and several outcomes that have a primary diagnosis as indicated. We use the Clinical Classifications Software (CCS) from the Agency for Healthcare Research and Quality (AHRQ) to classify the relevant ICD code groupings (around 250 groups), and plot the results for all CCS groupings where the mean of the outcome is at least 3.02, half the mean of our influenza outcome (6.04), to ensure there are enough cases in our outcome. The p-values are not adjusted for the family wise error rate. The associated q-values from a Holm-Bonferroni correction are all above 0.1 except for influenza as outcome.

Table A.8: Using instruments based on thermal inversions

	Only inversions		Wind and inversions	
	(1)	(2)	(3)	(4)
AQI	.012 (.029)	.29 (.1)	.029 (.0076)	.12 (.022)
AQI X VP		-1.4 (.44)		-.6 (.12)
Observations	17668	17668	17668	17668
Mean of outcome	6.04	6.04	6.04	6.04
Mean of AQI	35.27	35.27	35.27	35.27
Mean of VP	-	0.21	-	0.21
Mean of VE	-	0.36	-	0.36

Notes: The dependent variable is the count of inpatient hospitalizations with influenza as primary diagnosis in columns at the county-year-month level. We limit analysis to the influenza intensive months of October through March and our sample spans 2007-2017 with the exception of October 2008 to March 2009 where vaccine effectiveness data is not available. Vaccine protection (VP) is weighted by hospitalization shares across age groups and is measured between 0 (low) and 1 (high). The results are from a Poisson GMM estimation with county-by-season-by-year fixed effects and year-by-month dummies as well as weather controls. Weather controls consist of five bins of temperature quintiles, five bins of specific humidity quintiles, and linear terms for precipitation and wind speed. All weather variables are based on county-year-month averages. The air quality index (AQI) is lagged one month and a higher AQI means worse air quality. In Columns (1) and (2) we use our instruments based on thermal inversions instead of the AQI to generate moment conditions, and in Columns (3) and (4) we additionally use our instruments based on wind direction. In even-numbered columns we also use our VE instrument instead of VP to form moment conditions. Standard errors in parentheses are clustered at the county level.

Table A.9: Further robustness: Fixed effects, controls, AQI construction, and including off-seasonal cases

	Fewer FE		No weather ctr.		Incl. emp ctr.		AQI not wins.		AQI not interpol.		Incl. off-seas. cases	
	(1)	(2)	(3)	(4)	(5)	(6)	(7)	(8)	(9)	(10)	(11)	(12)
AQI	.025 (.0065)	.066 (.018)	.015 (.008)	.062 (.021)	.028 (.0074)	.11 (.025)	.028 (.0073)	.11 (.025)	.02 (.0081)	.091 (.026)	.011 (.0066)	.058 (.016)
AQI X VP		-.26 (.11)		-.32 (.15)		-.53 (.16)		-.58 (.15)		-.47 (.15)		-.27 (.071)
Observations	21459	21459	17668	17668	17665	17665	17668	17668	8950	8950	21702	21702
Mean of outcome	4.98	4.98	6.04	6.04	6.04	6.04	6.04	6.04	9.83	9.83	5.5	5.5
Mean of AQI	35.05	35.05	35.27	35.27	35.27	35.27	35.43	35.43	36.26	36.26	36.61	36.61
Mean of VP	-	0.21	-	0.21	-	0.21	-	0.21	-	0.21	-	0.21
Mean of VE	-	0.37	-	0.36	-	0.36	-	0.36	-	0.37	-	0.37

Notes: The dependent variable is the count of inpatient hospitalizations with influenza as primary diagnosis at the county-year-month level. We limit analysis to the influenza intensive months of October through March, except in Columns (11) and (12) where we also include all county-year-month cells with influenza cases between April and September. Our sample spans 2007-2017 with the exception of October 2008 to March 2009 where vaccine effectiveness data is not available. Vaccine protection (VP) is weighted by hospitalization shares across age groups and is measured between 0 (low) and 1 (high). The results are from a Poisson GMM estimation with county-by-season-by-year fixed effects (except Columns (1) and (2)) and year-by-month dummies as well as weather controls (except Columns (3) and (4)). Weather controls consist of five bins of temperature quintiles, five bins of specific humidity quintiles, and linear terms for precipitation and wind speed. All weather variables are based on county-year-month averages. The air quality index (AQI) is lagged one month and a higher AQI means worse air quality. In Columns (1) and (2), we include coarser fixed effects at the county-season level instead of at the county-season-year level. In Columns (3) and (4) we drop all weather controls. In Columns (5) and (6) we additionally include lagged employment counts at the county-year-month level. In Columns (7) and (8) we construct our AQI variable without winsorization at the top and bottom 1%. In Columns (9) and (10) we do not spatially interpolate, i.e. do not take the average value of the adjacent counties in the same month if the AQI is missing for certain county-year-month cells. All results use our instruments based on wind direction instead of the AQI to generate moment conditions, and in even-numbered columns additionally use our VE instrument instead of VP to form moment conditions. The number of included observations can vary across different outcomes due to fixed effects and varied counts in each county-year-month cell. Standard errors in parentheses are clustered at the county level.

Table A.10: Total hospitalization charges, length of stay, and charges per day (no instrument)

	Total charges				Length of stay in days				Charges per day			
	Linear (1)	GMM-IV (2)	Poisson (3)	GMM-IV (4)	Linear (5)	GMM-IV (6)	Poisson (7)	GMM-IV (8)	Linear (9)	GMM-IV (10)	Poisson (11)	GMM-IV (12)
AQI	1517 (839)	4906 (2289)	.0035 (.0025)	.035 (.0094)	.0066 (.0049)	.011 (.017)	.0028 (.0021)	.006 (.0063)	910 (426)	3181 (1151)	.0065 (.0024)	.039 (.0089)
AQI X VP		-16386 (8991)		-.16 (.045)		-.023 (.084)		-.015 (.03)		-11362 (4191)		-.17 (.042)
Observations	17754	17754	17754	17754	17783	17783	17783	17783	9689	9689	9689	9689
Mean of outcome	174095	174095	174095	174095	2.64	2.64	2.64	2.64	72119	72119	72119	72119
Mean of AQI	35.28	35.28	35.28	35.28	35.29	35.29	35.29	35.29	36.35	36.35	36.35	36.35
Mean of VP	-	0.21	-	0.21	-	0.21	-	0.21	-	0.21	-	0.21
Mean of VE	-	0.36	-	0.36	-	0.36	-	0.36	-	0.36	-	0.36

Notes: The dependent variable are hospital charges for inpatient hospitalizations with influenza as primary diagnosis, length of stay in days, or charges per day. We limit analysis to the influenza intensive months of October through March and our sample spans 2007-2017 with the exception of October 2008 to March 2009 where vaccine effectiveness data is not available. Vaccine protection (VP) is weighted by hospitalization shares across age groups and is measured between 0 (low) and 1 (high). The results are from a Linear GMM estimation and from a Poisson GMM estimation as indicated, all with county-by-season-by-year fixed effects and year-by-month dummies as well as weather controls. Weather controls consist of five bins of temperature quintiles, five bins of specific humidity quintiles, and linear terms for precipitation and wind speed. All weather variables are based on county-year-month averages. The air quality index (AQI) is lagged one month and a higher AQI means worse air quality. All results are based on moment conditions without using any instruments. Standard errors in parentheses are clustered at the county level.

REFERENCES

- CDC (2020), *U.S. Outpatient Influenza-like Illness Surveillance Network (ILINet)*, Centers for Disease Control and Prevention.
- EPA (2018), *Technical Assistance Document for the Reporting of Daily Air Quality*, United States Environmental Protection Agency.
- EPA (2020), *Air Quality System Data Mart*, US Environmental Protection Agency.
- HCUP (2018), *HCUP State Inpatient Databases (SID)*, Healthcare Cost and Utilization Project, Agency for Healthcare Research and Quality, Rockville, MD.